

Dibenzocyclooctadiene Lignans from *Schisandra chinensis* with Anti-inflammatory Effects

Michal Rybníkář ^{1,*}, Milan Malaník ¹, Karel Šmejkal ¹, Emil Švajdlenka ¹, Polina Shpet ^{1,2}, Pavel Babica², Stefano Dall'Acqua ³, Ondřej Smištík ⁴, Ondřej Jurček ¹, and Jakub Treml ^{4,*}

Supplementary data

List of figures:

- Figure S1. ¹H NMR spectrum of compound **1** in CD₃OD-*d*₄ (at 303 K)
Figure S2. HSQCDEPT NMR spectrum of compound **1** in CD₃OD-*d*₄ (at 303 K)
Figure S3. HMBC NMR spectrum of compound **1** in CD₃OD-*d*₄
Figure S4. Diagnostic HMBC correlations of compound **1** in CD₃OD-*d*₄
Figure S5. COSY NMR spectrum of compound **1** in CD₃OD-*d*₄
Figure S6. NOESY NMR spectrum of compound **1** in CD₃OD-*d*₄
Figure S7. HPLC-ELSD chromatogram of compound **1**
Figure S8. UV spectrum of compound **1**
Figure S9. LC-MS and HRMS spectrum of compound **1**
Figure S10. ¹H NMR spectrum of compound **2** in CDCl₃-*d*
Figure S11. HMBC NMR spectrum of compound **2** in CDCl₃-*d*
Figure S12. HQSC NMR spectrum of compound **2** in CDCl₃-*d*
Figure S13. COSY NMR spectrum of compound **2** in CDCl₃-*d*
Figure S14. NOESY NMR spectrum of compound **2** in CDCl₃-*d*
Figure S15. HPLC-DAD chromatogram of compound **2**
Figure S16. LR-MS spectrum of compound **2**
Figure S17. CD spectrum of compound **2**
Figure S18. IR spectrum of compound **2**
Figure S19. ¹H NMR spectrum of compound **3** in CDCl₃-*d*
Figure S20. HMBC NMR spectrum of compound **3** in CDCl₃-*d*
Figure S21. HSQC NMR spectrum of compound **3** in CDCl₃-*d*
Figure S22. COSY NMR spectrum of compound **3** in CDCl₃-*d*
Figure S23. NOESY NMR spectrum of compound **3** in CDCl₃-*d*
Figure S24. HPLC-DAD chromatogram of compound **3**
Figure S25. LR-MS spectrum of compound **3**
Figure S26. CD spectrum of compound **3**
Figure S27. IR spectrum of compound **3**
Figure S28. ¹H NMR spectrum of compound **4** in CD₃OD-*d*₄
Figure S29. HMBC NMR spectrum of compound **4** in CD₃OD-*d*₄
Figure S30. HSQC NMR spectrum of compound **4** in CD₃OD-*d*₄
Figure S31. COSY NMR spectrum of compound **4** in CD₃OD-*d*₄
Figure S32. NOESY NMR spectrum of compound **4** in CD₃OD-*d*₄
Figure S33. HPLC-DAD chromatogram of compound **4**
Figure S34. LR-MS chromatogram of compound **4**
Figure S35. CD spectrum of compound **4**
Figure S36. IR spectrum of compound **4**
Figure S37. ¹H NMR spectrum of compound **5** in CD₃OD-*d*₄
Figure S38. HMBC NMR spectrum of compound **5** in CD₃OD-*d*₄
Figure S39. HSQC NMR spectrum of compound **5** in CD₃OD-*d*₄
Figure S40. COSY NMR spectrum of compound **5** in CD₃OD-*d*₄
Figure S41. NOESY NMR spectrum of compound **5** in CD₃OD-*d*₄
Figure S42. HPLC-DAD chromatogram of compound **5**
Figure S43. LR-MS spectrum of compound **5**
Figure S44. CD spectrum of compound **5**
Figure S45. IR spectrum of compound **5**

Figure S46. HPLC-DAD chromatogram of common injection of compound **6** with standard of (+)-deoxyschisandrin; UV spectrum of peak corresponding to (+)-deoxyschisandrin.

Figure S47. HPLC-DAD chromatogram of common injection of (-)-wuweizisu C with standard of (-)-wuweizisu C; UV spectrum of peak corresponding to (-)-wuweizisu C.

Figure S48. ¹H NMR spectrum of epigomisin O in CDCl₃-*d*

Figure S49. HMBC NMR spectrum of epigomisin O in CDCl₃-*d*

Figure S50. HSQC NMR spectrum of epigomisin O in CDCl₃-*d*

Figure S51. COSY NMR spectrum of epigomisin O in CDCl₃-*d*

Figure S52. NOESY NMR spectrum of epigomisin O in CDCl₃-*d*

Figure S53. HPLC-DAD chromatogram of epigomisin O

Figure S54. LR-MS spectrum of epigomisin O

Figure S55. CD spectrum of epigomisin O

Figure S56. IR spectrum of epigomisin O

Figure S57. ¹H NMR spectrum of arisantetralone C in CD Cl₃-*d*

Figure S58. HMBC NMR spectrum of arisantetralone C in CDCl₃-*d*

Figure S59. HSQC NMR spectrum of arisantetralone C in CDCl₃-*d*

Figure S60. COSY NMR spectrum of arisantetralone C in CDCl₃-*d*

Figure S62. NOESY NMR spectrum of arisantetralone C in CDCl₃-*d*

Figure S63. HPLC-DAD chromatogram of arisantetralone C

Figure S64. LR-MS spectrum of arisantetralone C

Figure S65. CD spectrum of arisantetralone C

Figure S66. IR spectrum of arisantetralone C

Figure S67. ¹H NMR spectrum of arisantetralone A in DMSO-*d*₆

Figure S68. HMBC NMR spectrum of arisantetralone A in DMSO-*d*₆

Figure S69. HSQC NMR spectrum of arisantetralone A in DMSO-*d*₆

Figure S70. COSY NMR spectrum of arisantetralone A in DMSO-*d*₆

Figure S71. NOESY NMR spectrum of arisantetralone A in DMSO-*d*₆

Figure S72. HPLC-DAD chromatogram of arisantetralone A

Figure S73. LR-MS spectrum of arisantetralone A

Figure S74. CD spectrum of arisantetralone A

Figure S75. IR spectrum of arisantetralone A

Figure S76. ¹H NMR spectrum of (-)-schisantherin E in DMSO-*d*₆

Figure S77. HMBC NMR spectrum of (-)-schisantherin E in DMSO-*d*₆

Figure S78. HSQC NMR spectrum of (-)-schisantherin E in DMSO-*d*₆

Figure S79. COSY NMR spectrum of (-)-schisantherin E in DMSO-*d*₆

Figure S80. HPLC-DAD chromatogram of (-)-schisantherin E

Figure S81. LR-MS spectrum of (-)-schisantherin E

Figure S82. CD spectrum of (-)-schisantherin E

Figure S83. IR spectrum of (-)-schisantherin E

Figure S84. Schema of isolation and total yields of compounds **2–6**, (-)-wuweizisu C, arisantetralone A, arisantetralone C, epigomisin O, and (-)-schisantherin E

Figure S85. Schema of isolation and yield of compound **1**

Figure S86. Antiproliferative activity of lignans **2–14**

Table S1. Chromatographic conditions of separation of compounds **2**, **6** and arisantetralone C from fraction SC 122-123

Table S2. Chromatographic conditions of separation of compounds **3**, **4**, **5** and **6** from fraction SC 130

Table S3. Chromatographic conditions of purification of compound **3** from fraction SC 130

Table S4. Chromatographic conditions of the first purification of compounds **4** and **5** from fraction SC 130

Table S5. Chromatographic conditions of the second purification of compounds **4** and **5** from fraction SC 130

Table S6. Chromatographic conditions of separation of compound **6** and (-)-wuweizisu C from fraction SC 120-121

Table S7. Chromatographic conditions of separation of epigomisin O from fraction SC 138-148

Table S8. Chromatographic conditions of separation of arisantetralone A from fraction SC 149-167

Table S9. Chromatographic conditions of separation of (-)-schisantherin E from fraction SC 175-181

Table S10. Chromatographic conditions of separation of compounds **3**, **4**, **5** and **6** from fraction SC 126-129

Table S11. Chromatographic conditions of purification of compounds **4** and **5** from fraction SC 126-129

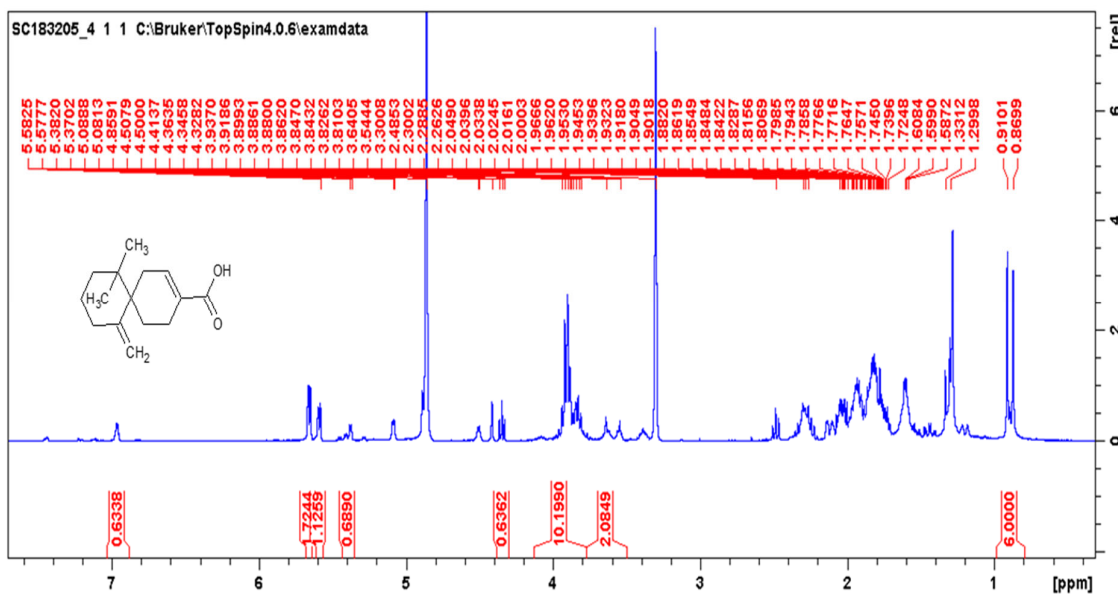


Figure S1. ¹H NMR spectrum of compound 1 in CD₃OD (at 303 K)

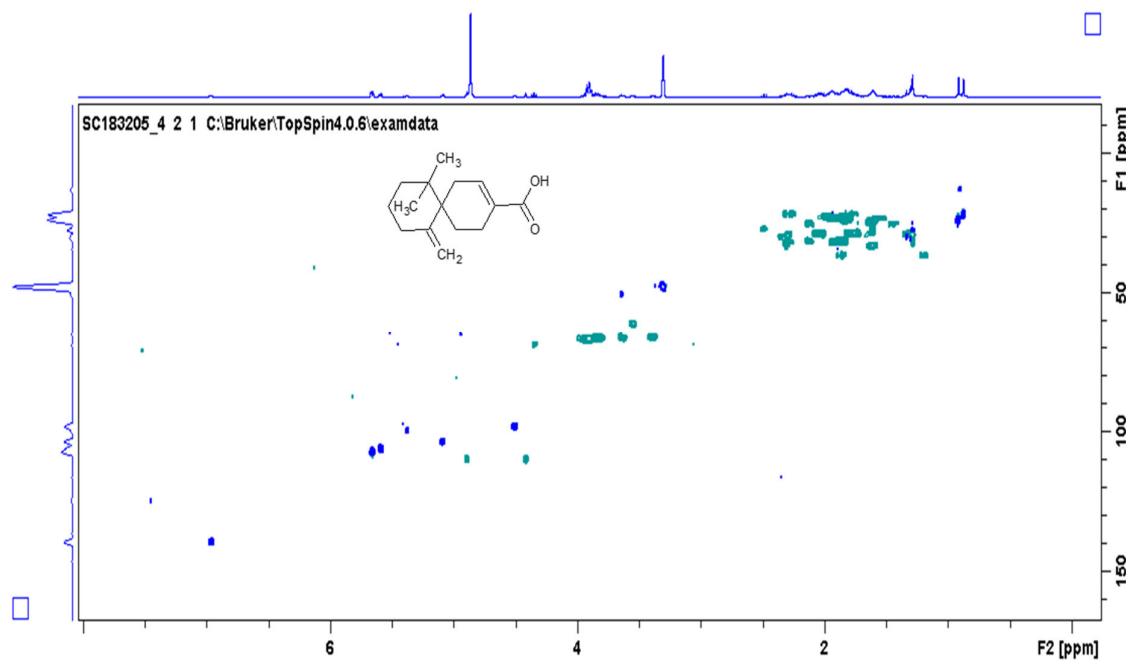


Figure S2. HSQCDEPT NMR spectrum of compound 1 in CD₃OD (at 303 K)

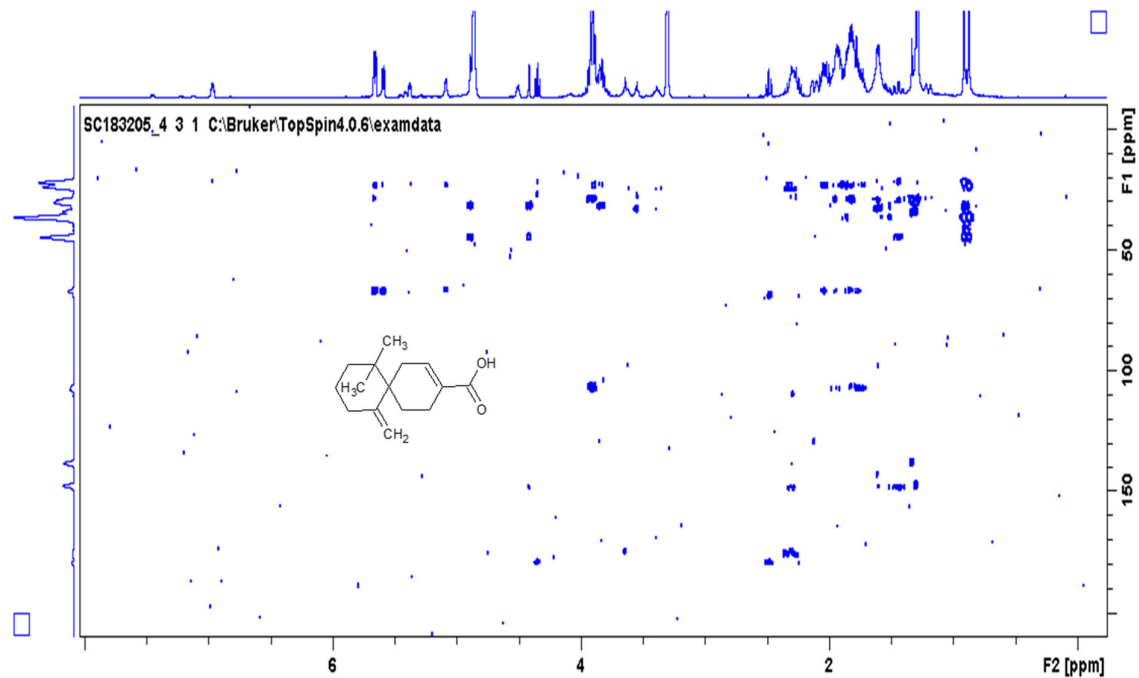


Figure S3. HMBC NMR spectrum of compound **1** in CD_3OD

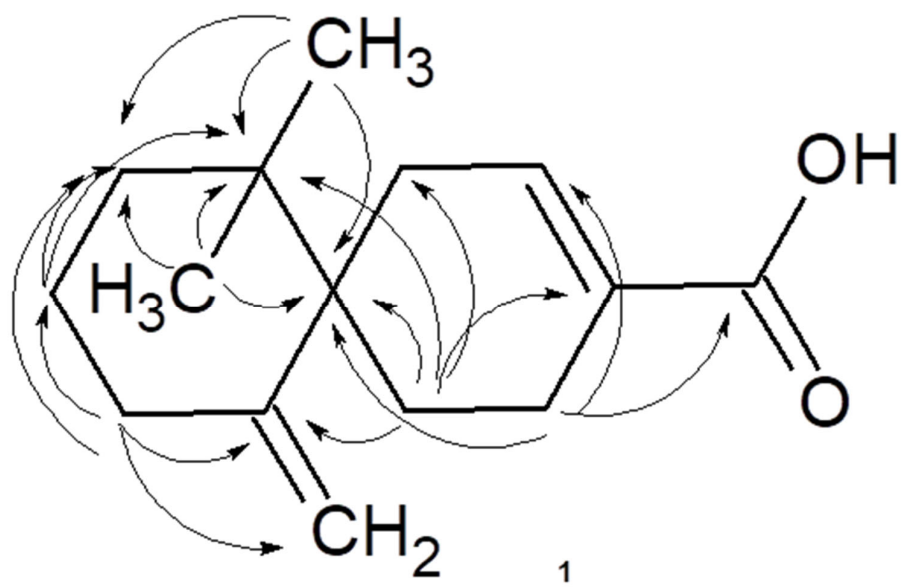


Figure S4. Diagnostic HMBC correlations of compound **1** in CD_3OD

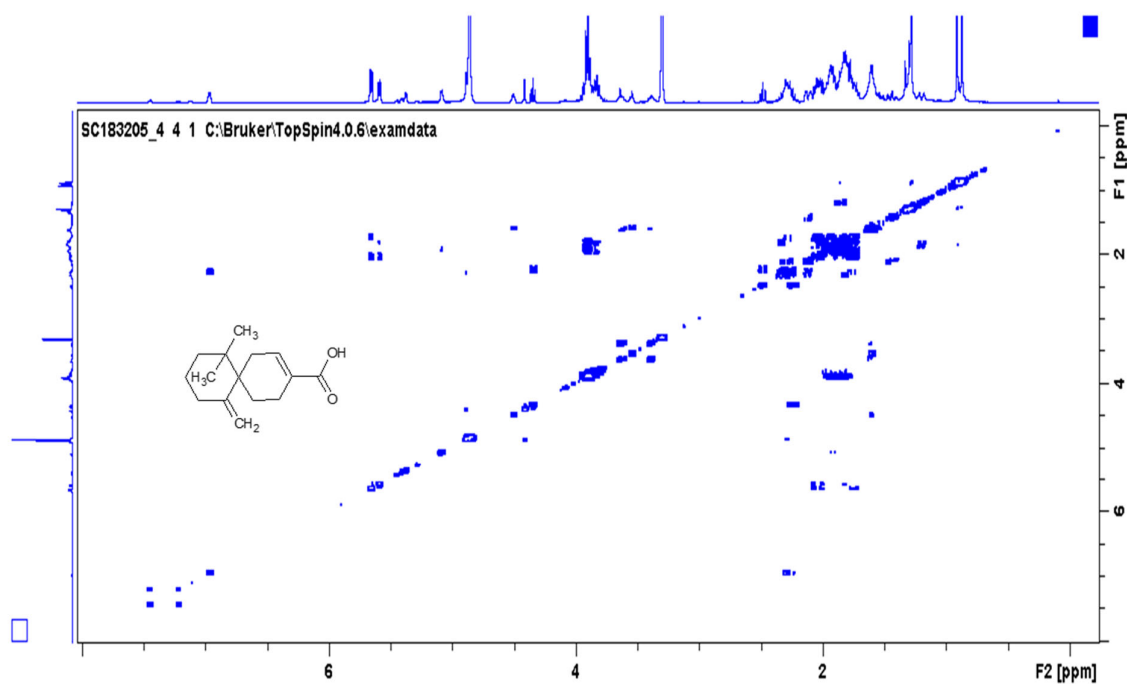


Figure S5. COSY NMR spectrum of compound **1** in CD_3OD

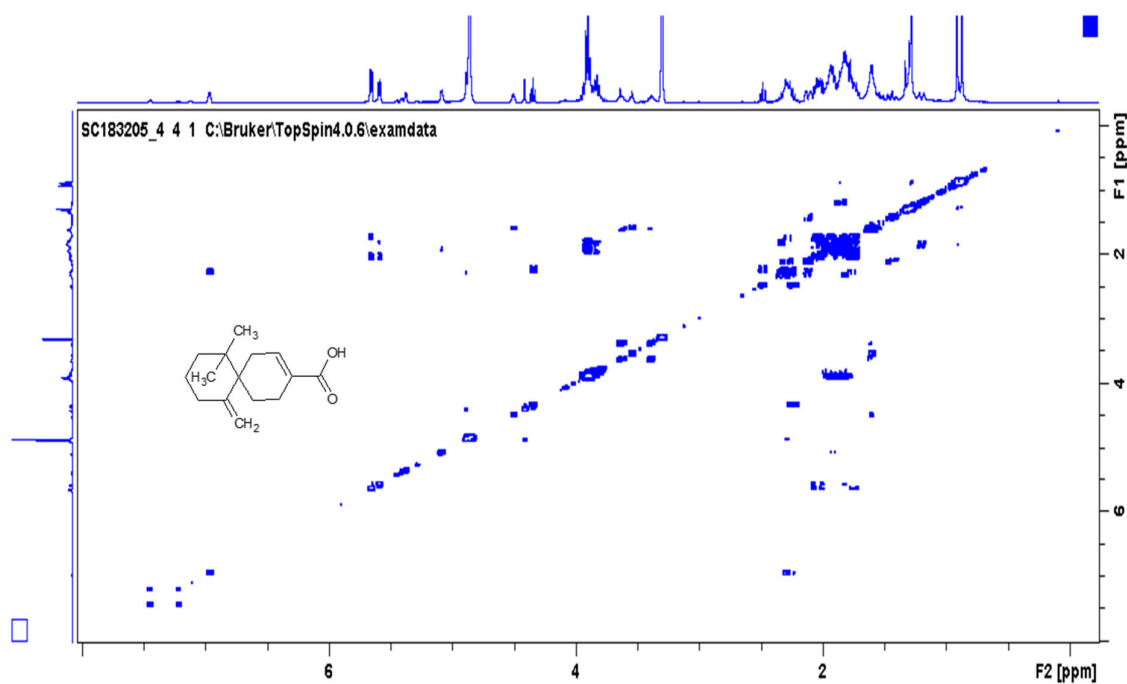


Figure S6. NOESY NMR spectrum of compound **1** in CD_3OD

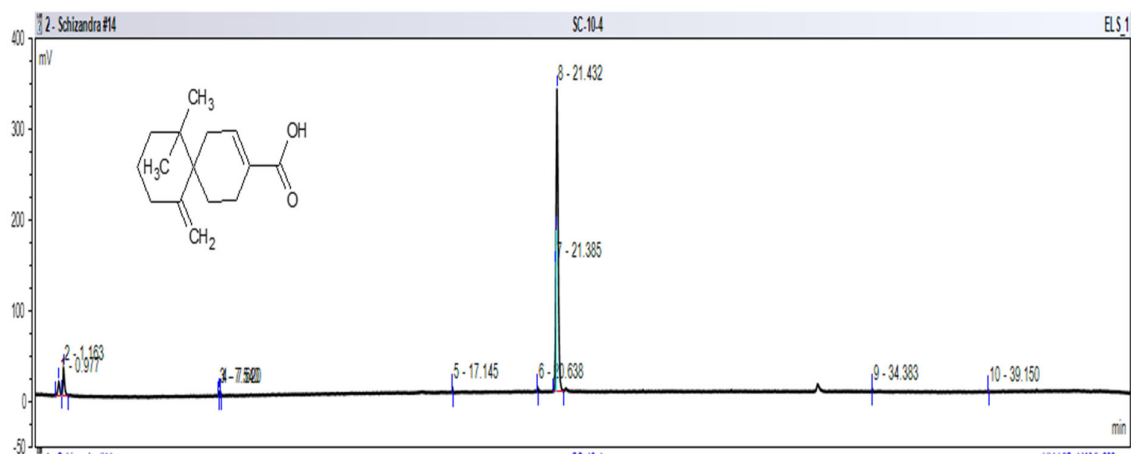


Figure S7. HPLC-ELSD chromatogram of compound 1

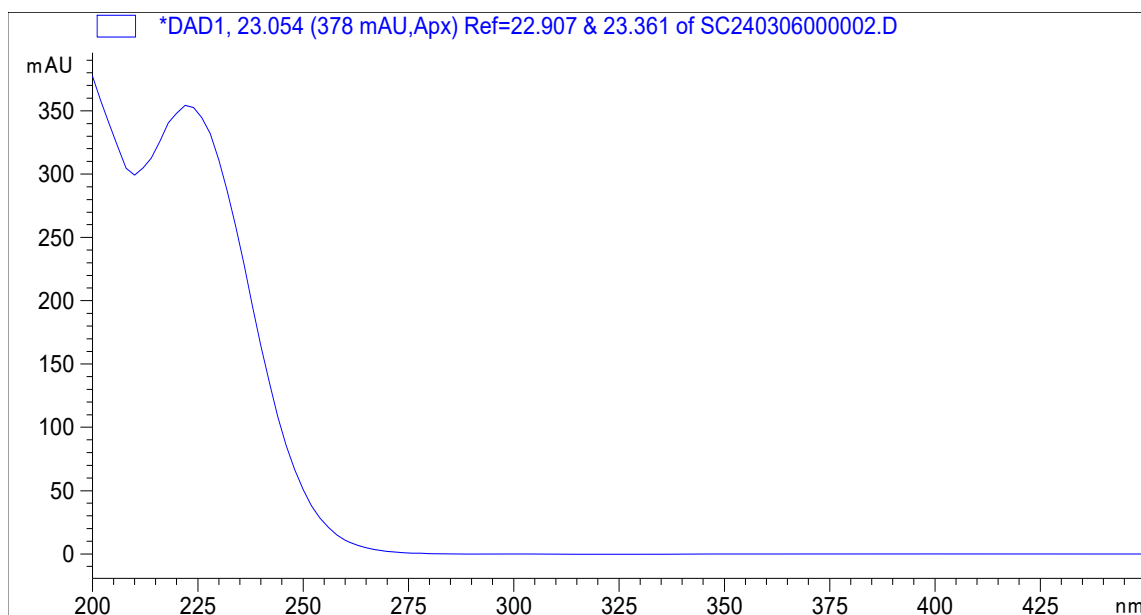


Figure S8. UV spectrum of compound 1

Expected Compounds per File

05-Mar-2024 1:21

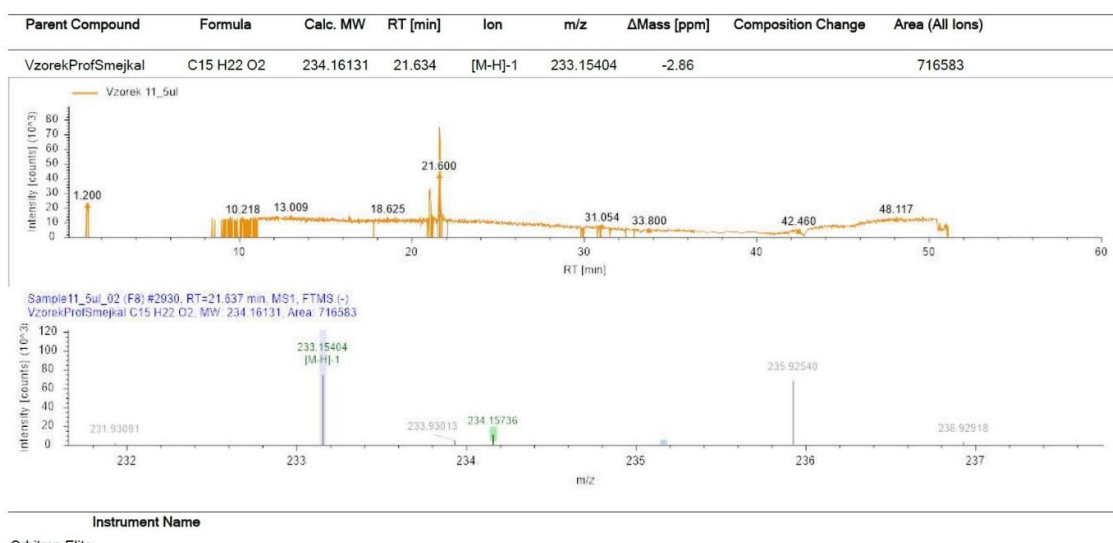


Figure S9. LC-MS and HRMS spectrum of compound 1

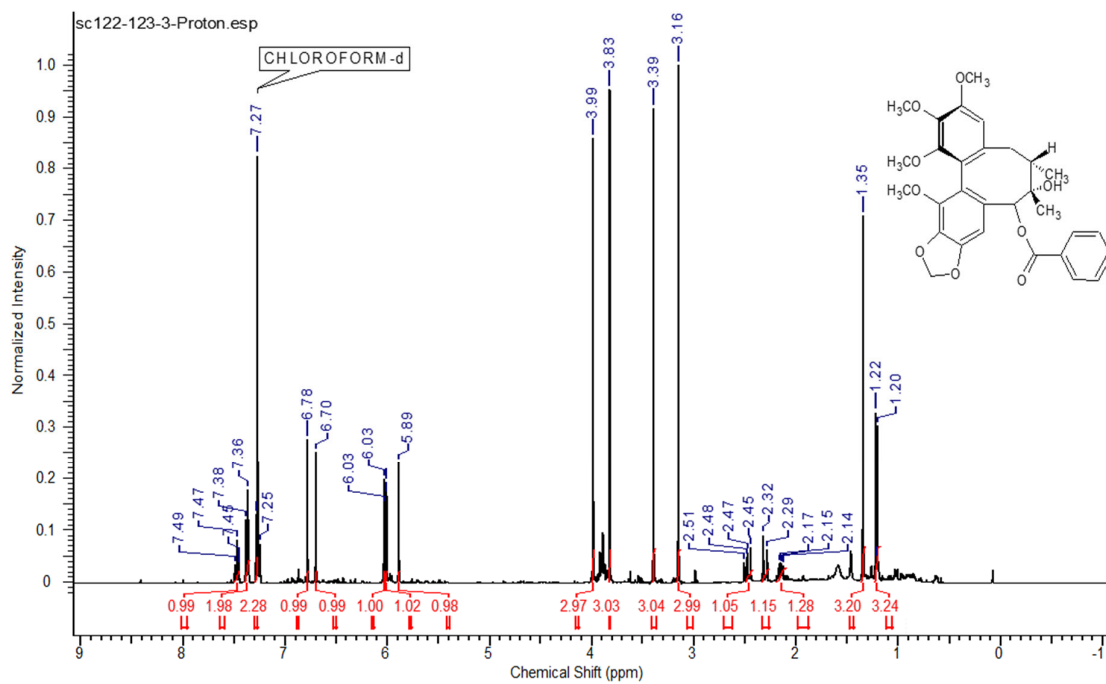


Figure S10. ^1H NMR spectrum of compound **2** in CDCl_3

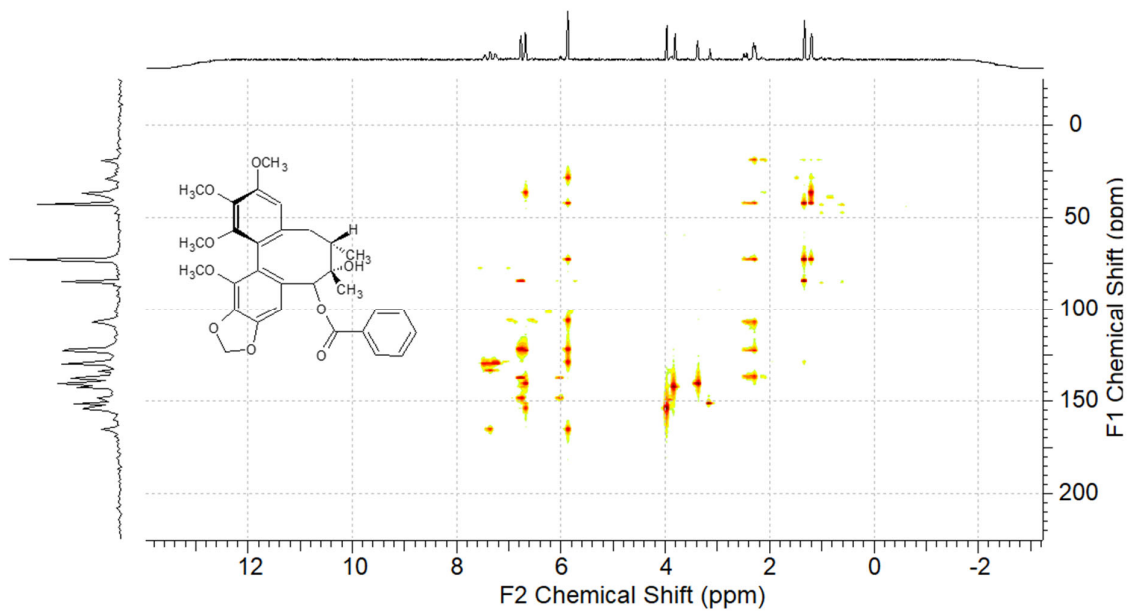


Figure S11. HMBC NMR spectrum of compound 2 in CDCl_3

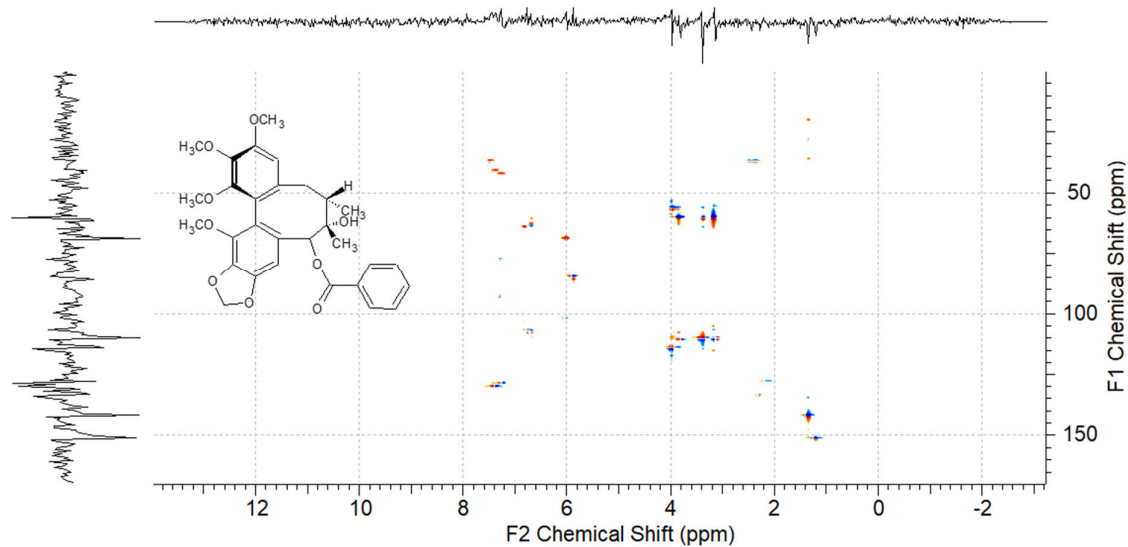


Figure S12. HQSC NMR spectrum of compound 2 in CDCl_3

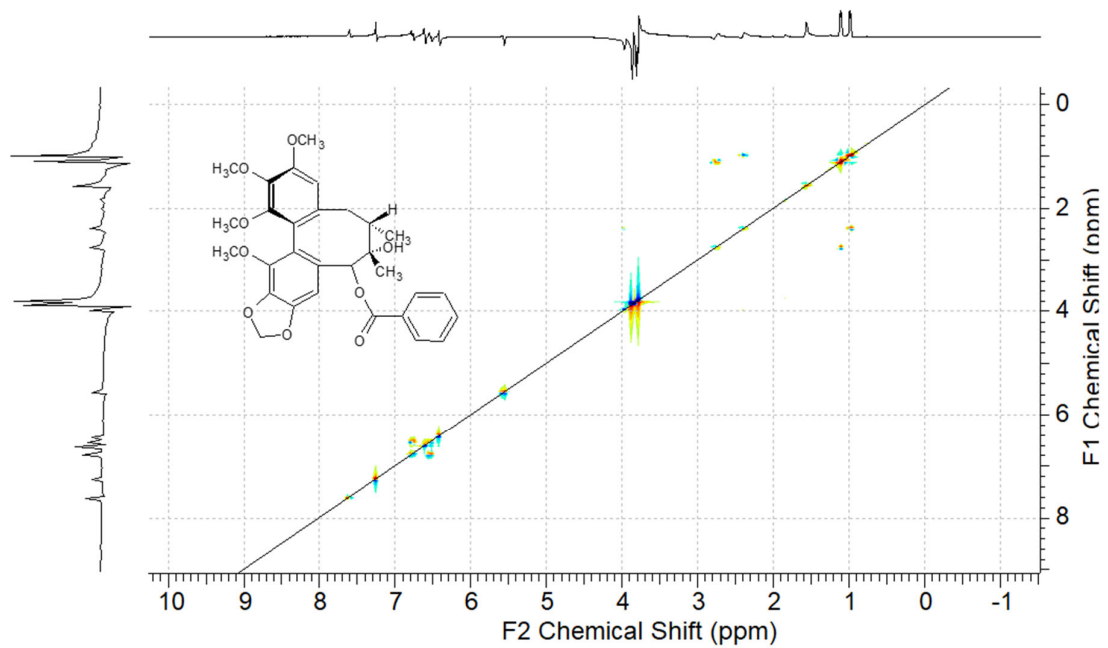


Figure S13. COSY NMR spectrum of compound **2** in CDCl_3

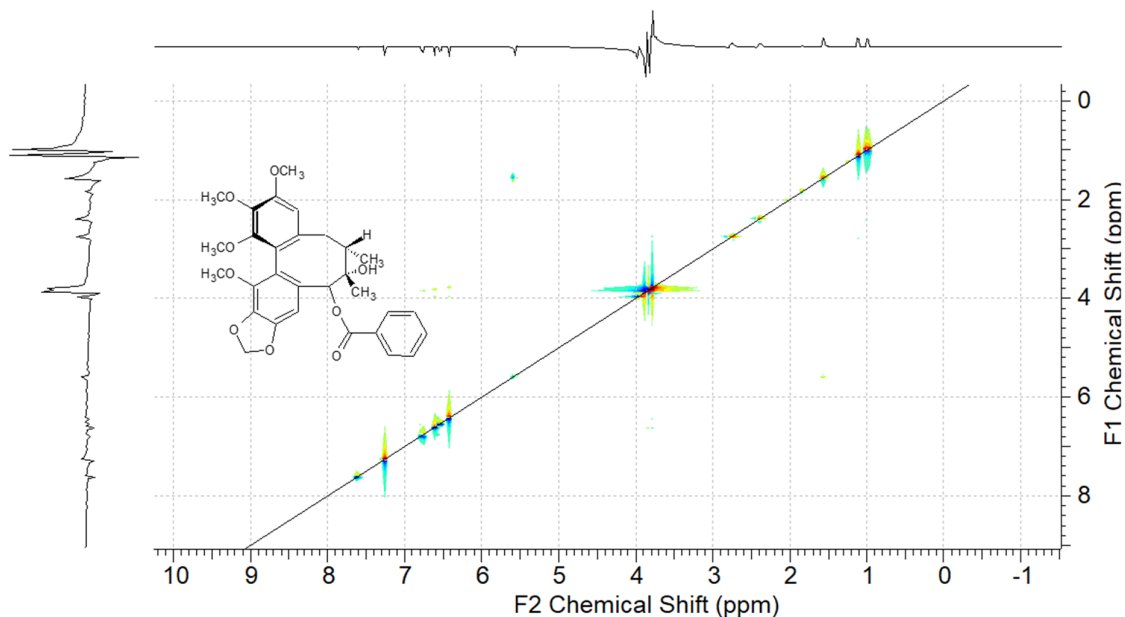


Figure S14. NOESY NMR spectrum of compound **2** in CDCl_3

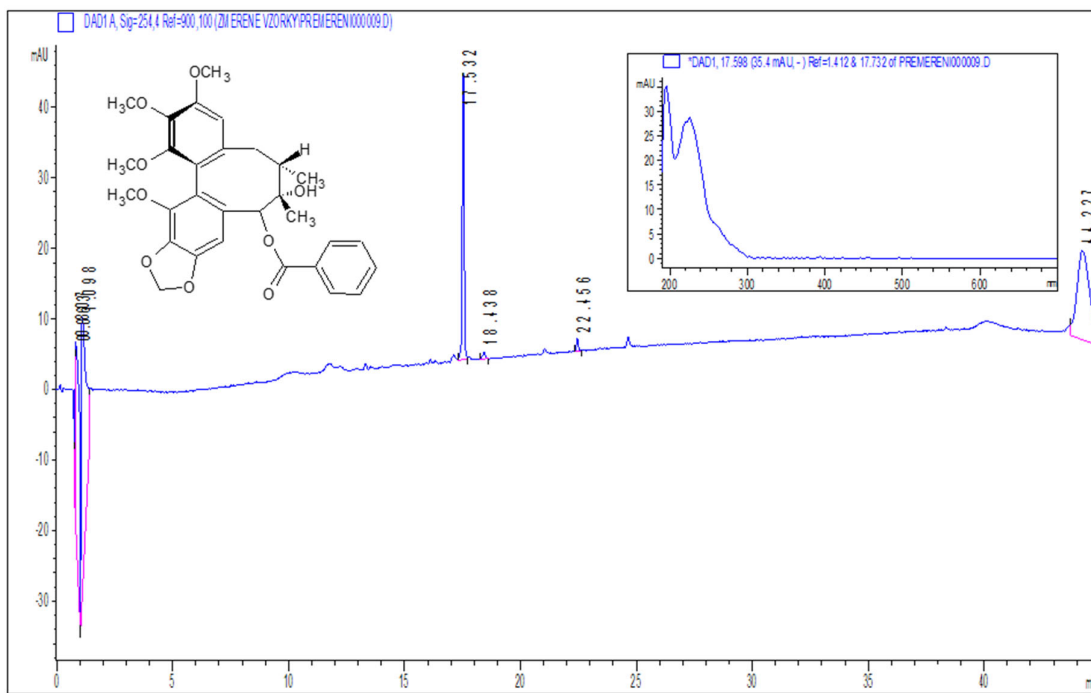


Figure S15. HPLC-DAD chromatogram of compound 2

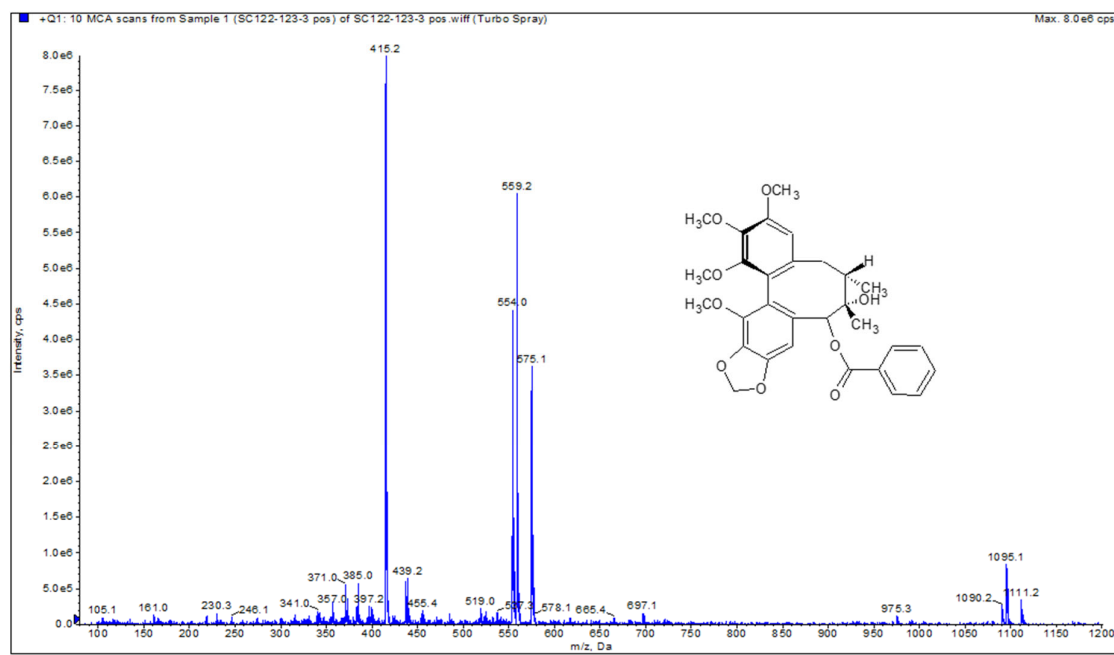


Figure S16. LR-MS spectrum of compound 2

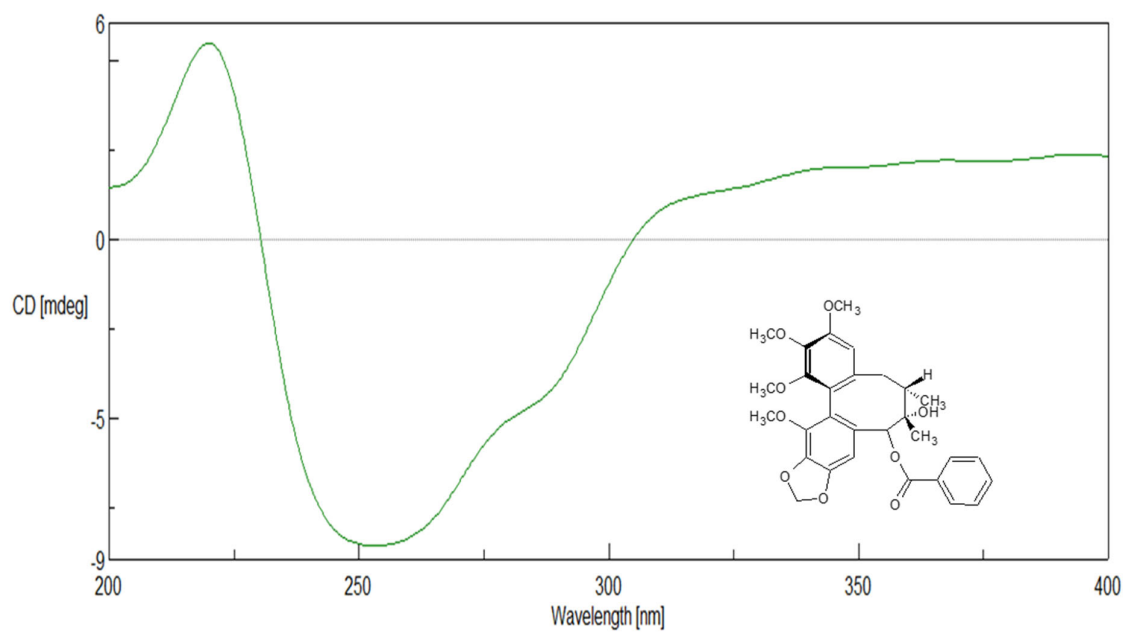


Figure S17. CD spectrum of compound **2** in methanol ($c = 1 \text{ mg/mL}$)

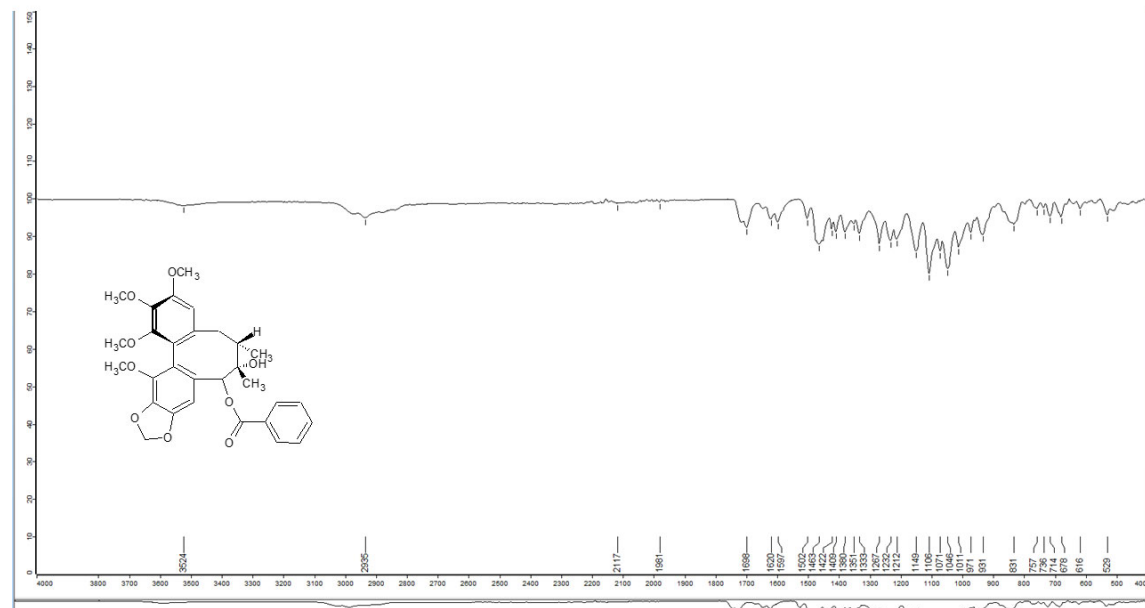


Figure S18. IR spectrum of compound **2**

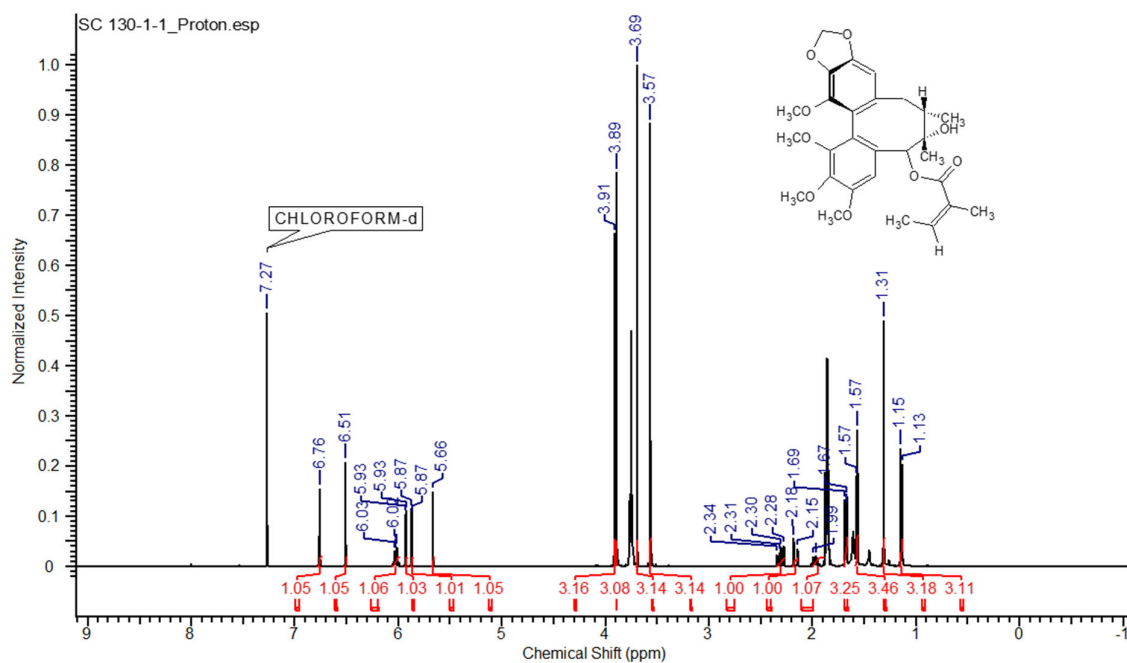


Figure S19. ^1H NMR spectrum of compound 3 in CDCl_3

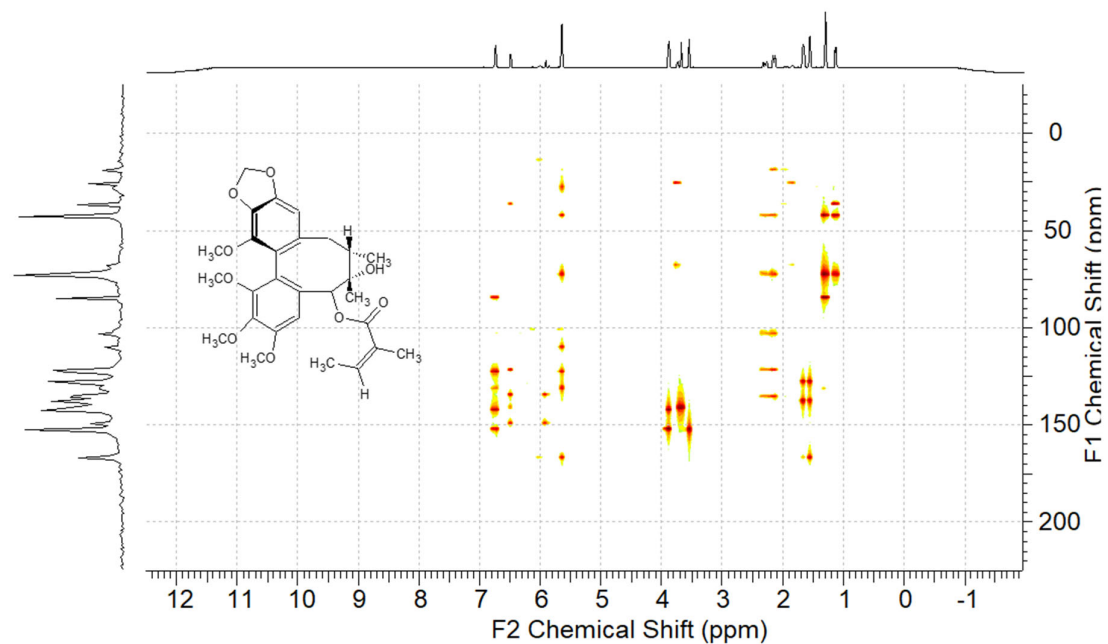


Figure S20. HMBC NMR spectrum of compound 3 in CDCl_3

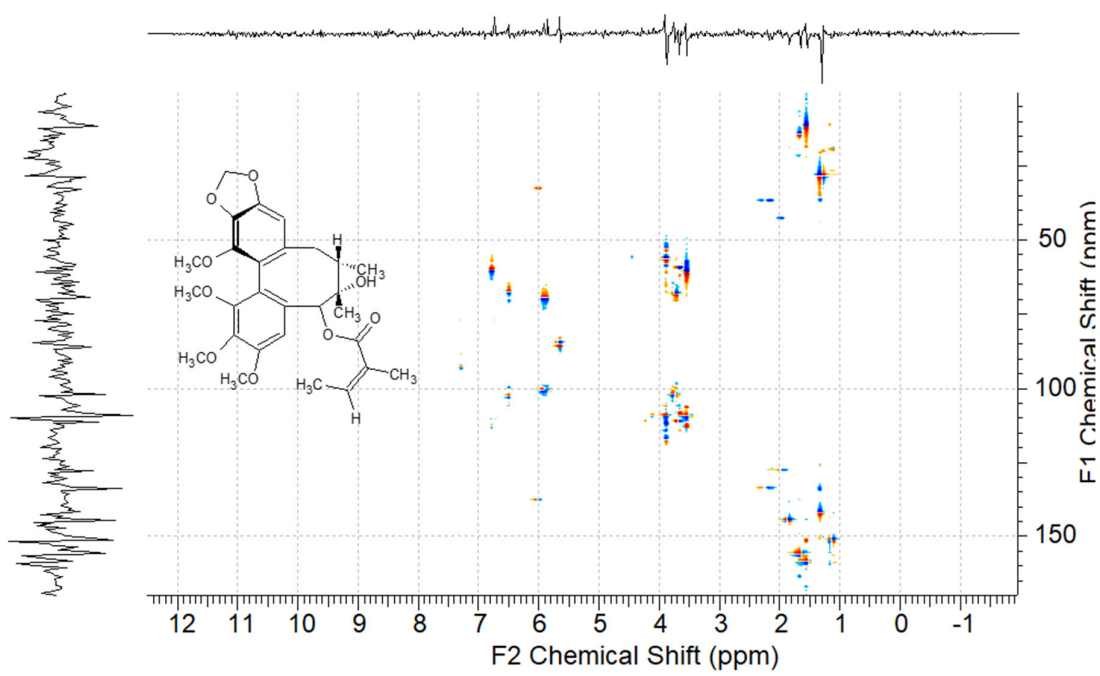


Figure S21. HSQC NMR spectrum of compound 3 in CDCl_3

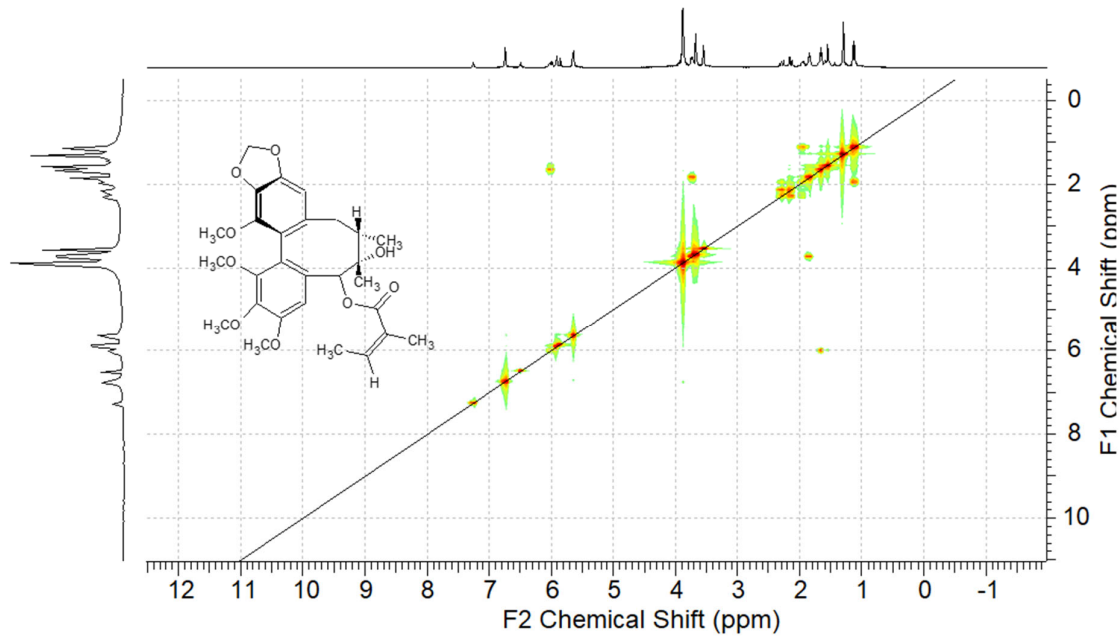


Figure S22. COSY NMR spectrum of compound 3 in CDCl_3

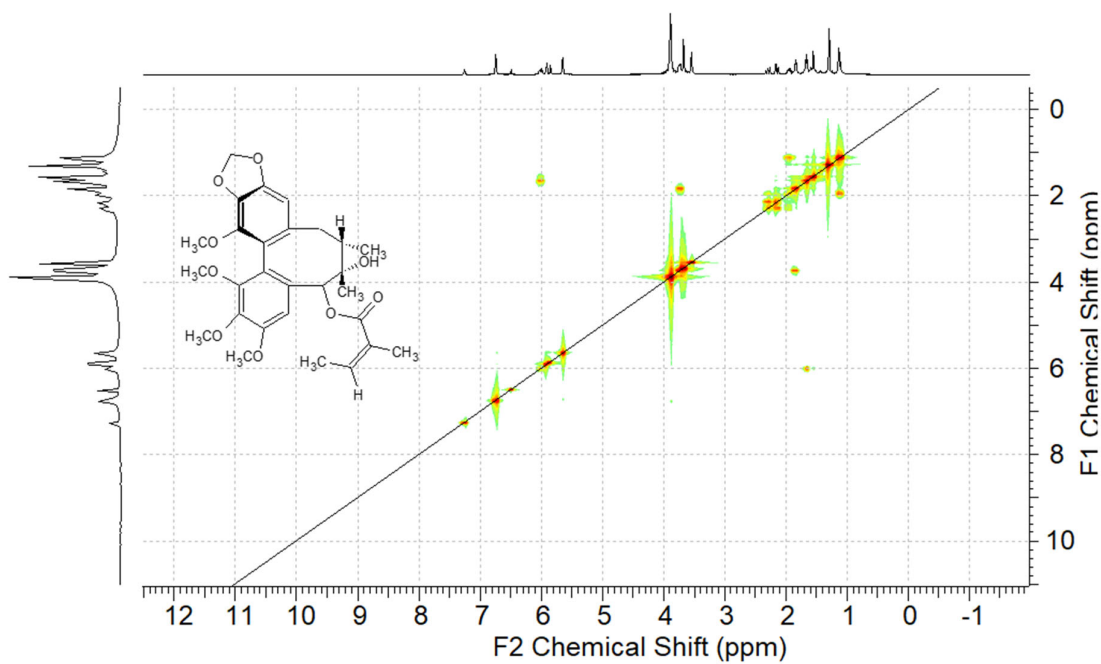


Figure S23. NOESY NMR spectrum of compound 3 in CDCl_3

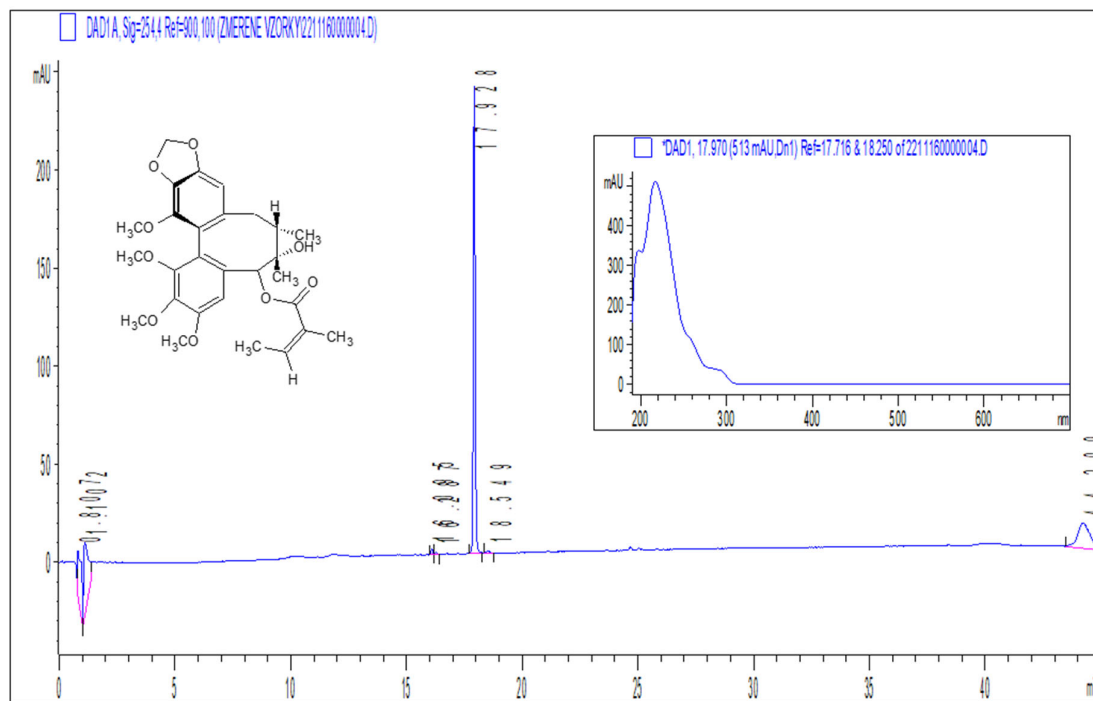


Figure S24. HPLC-DAD chromatogram of compound 3

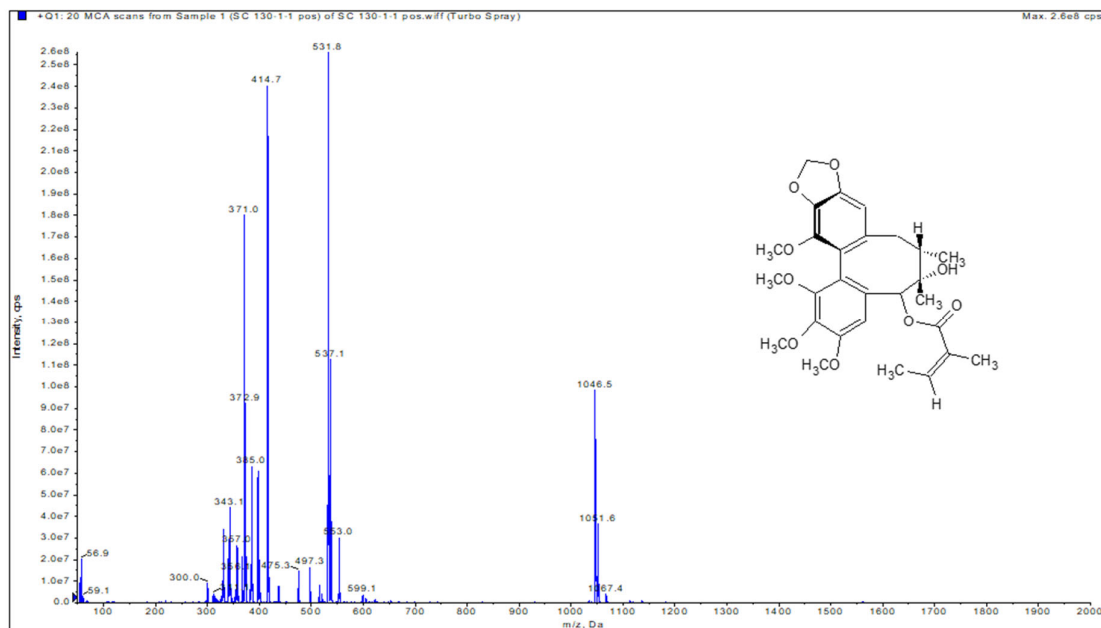


Figure S25. LR-MS spectrum of compound 3

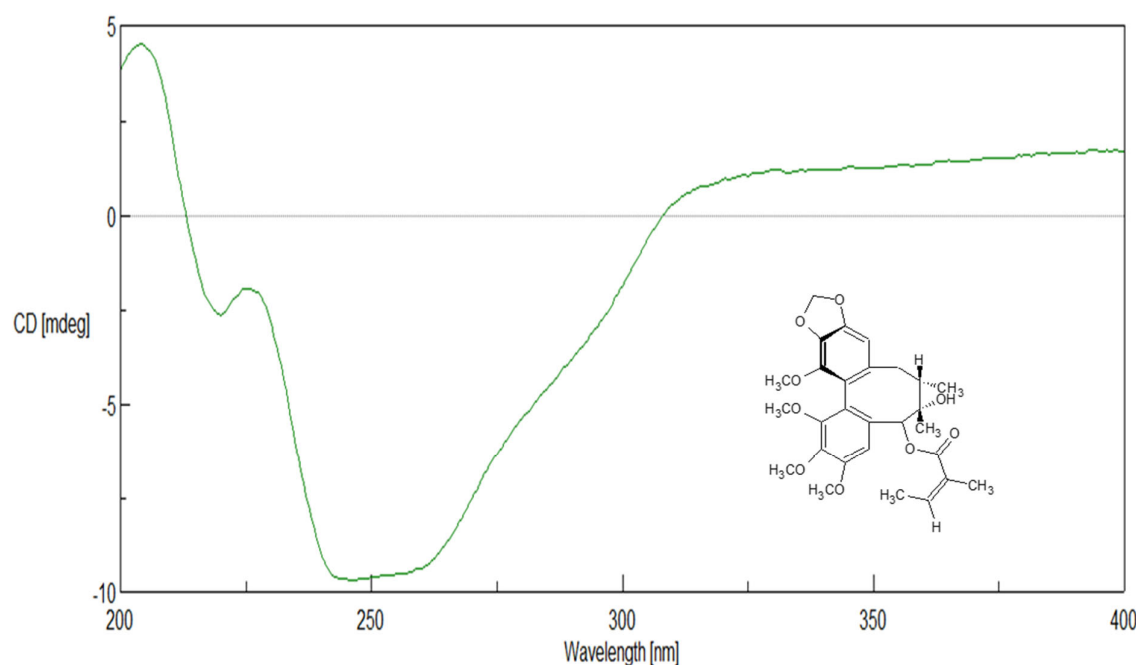


Figure S26. CD spectrum of compound **3** in methanol ($c=1$ mg/mL)

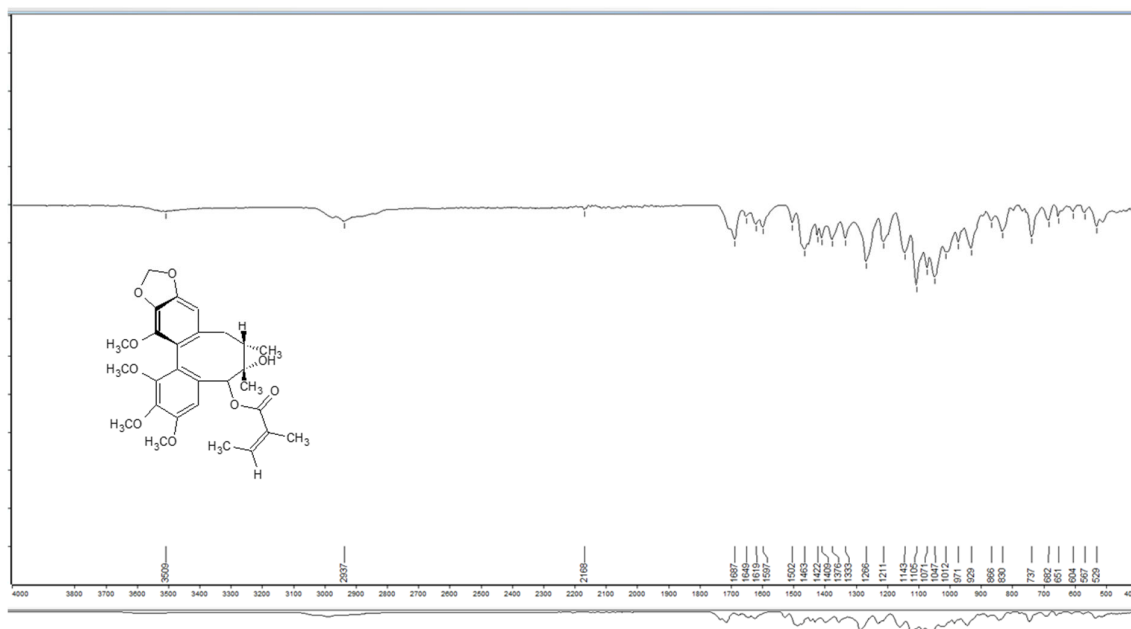


Figure S27. IR spectrum of compound 3

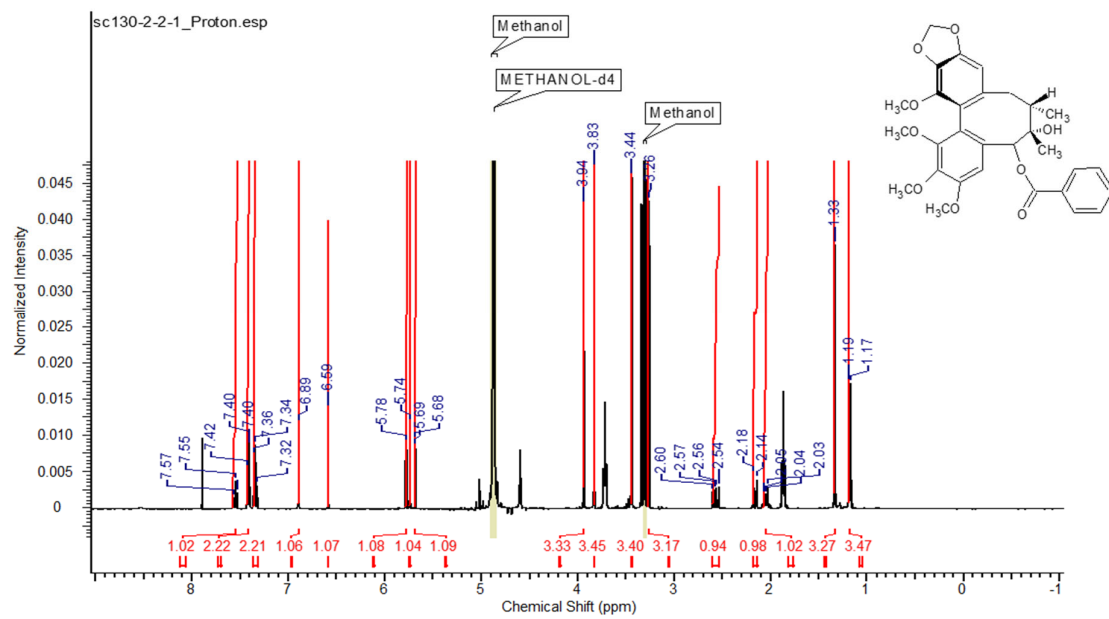


Figure S28. ¹H NMR spectrum of compound 4 in CD₃OD

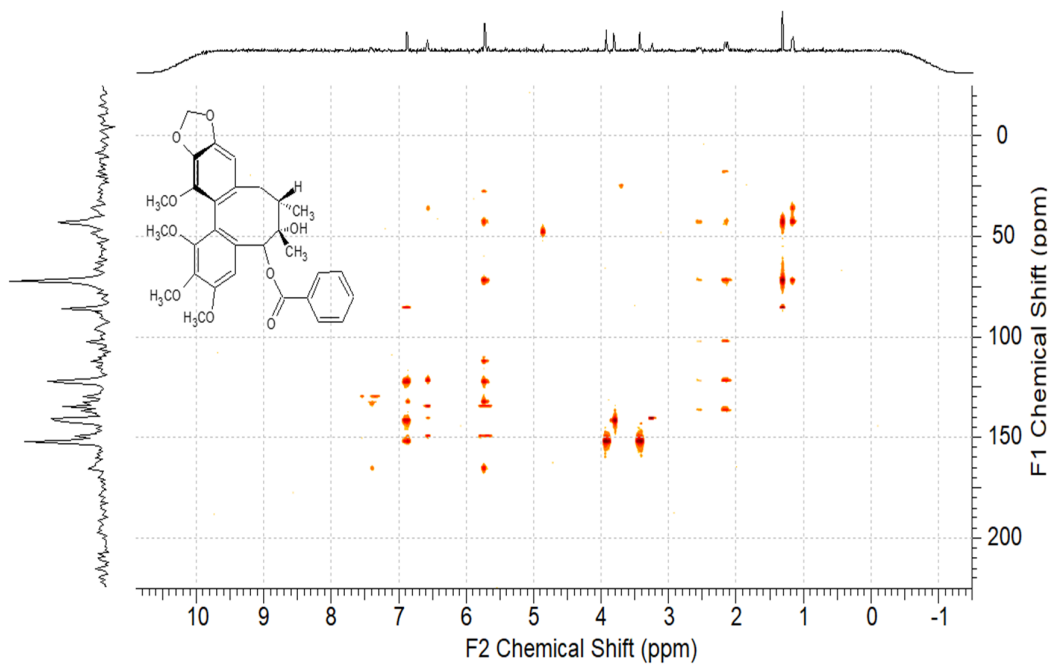


Figure S29. HMBC NMR spectrum of compound 4 in CD_3OD

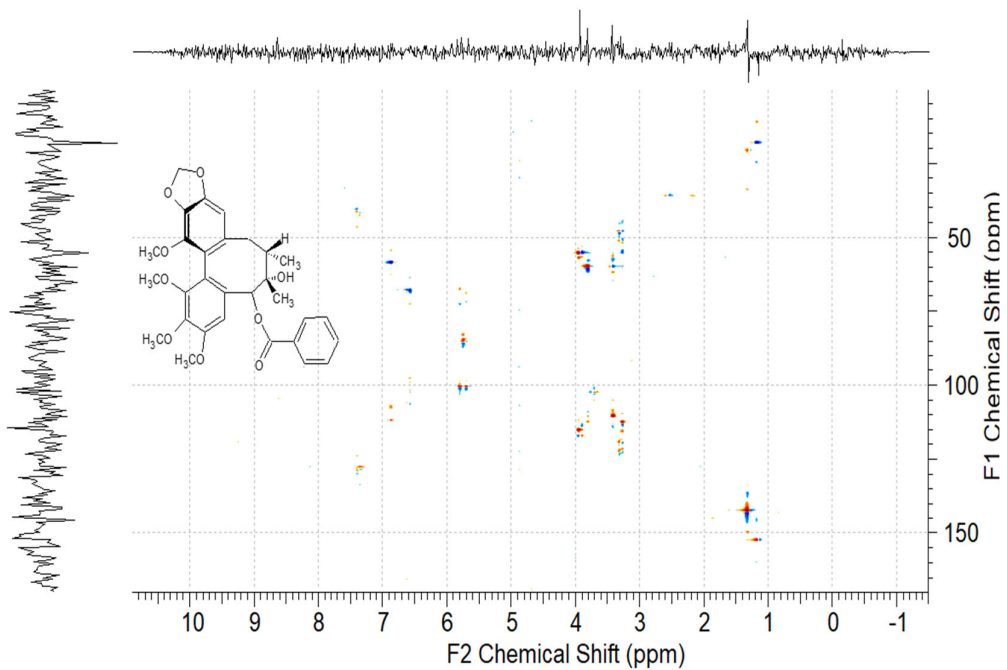


Figure S30. HSQC NMR spectrum of compound 4 in CD_3OD

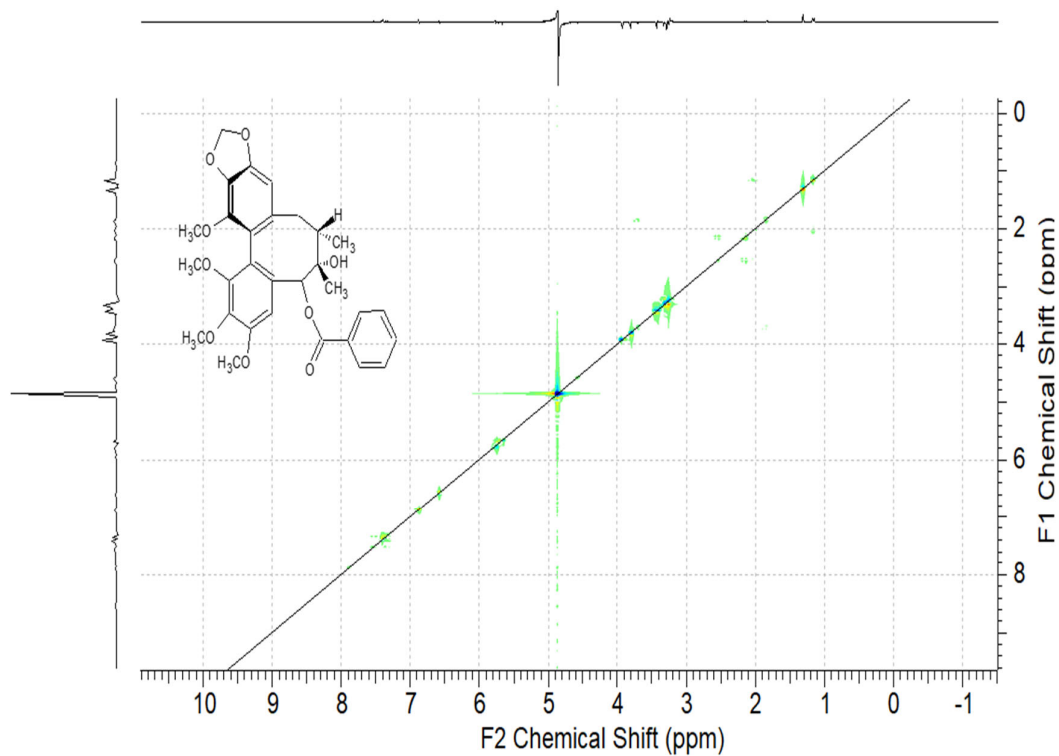


Figure S31. COSY NMR spectrum of compound **4** in CD_3OD

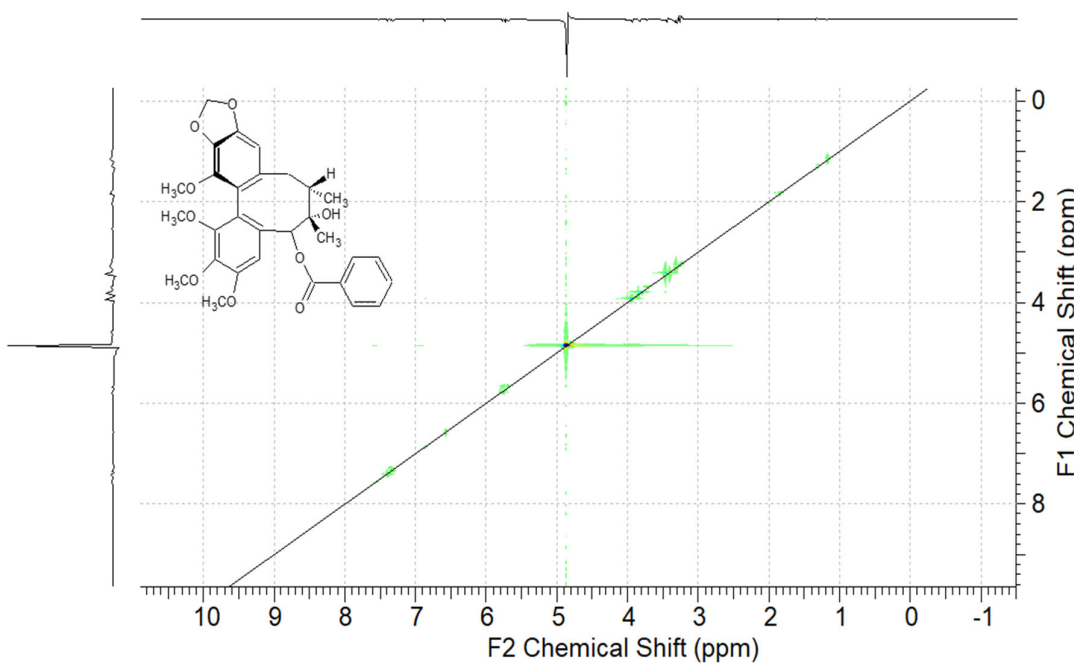


Figure S32. NOESY NMR spectrum of compound **4** in CD_3OD

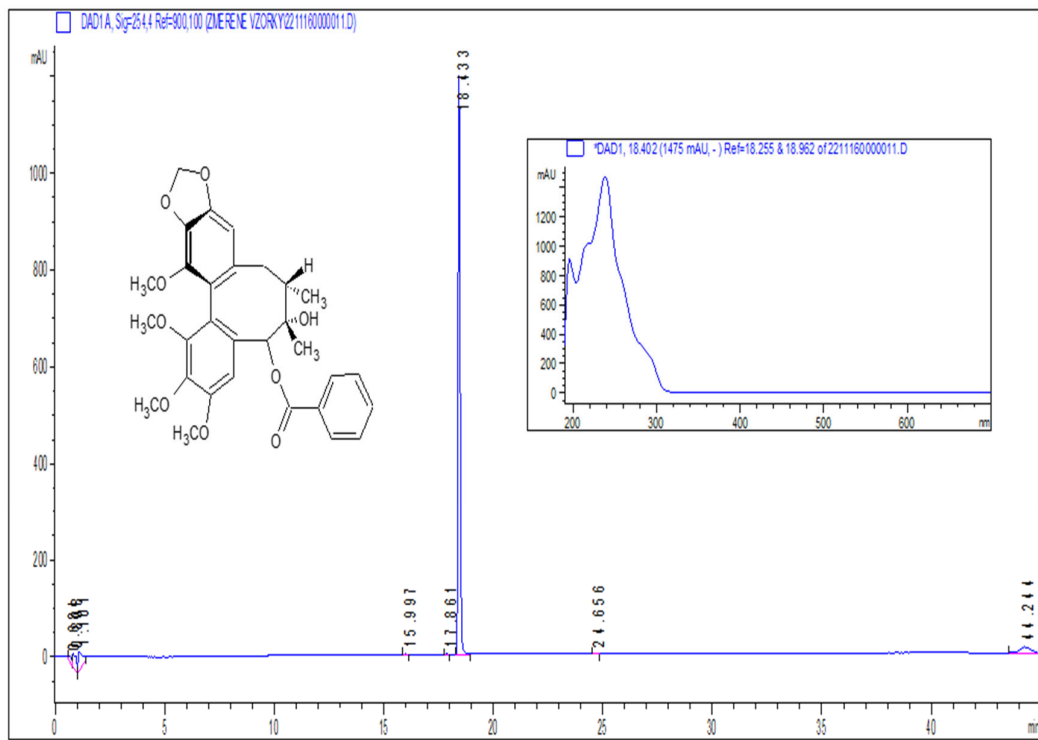


Figure S33. HPLC-DAD chromatogram of compound **4**

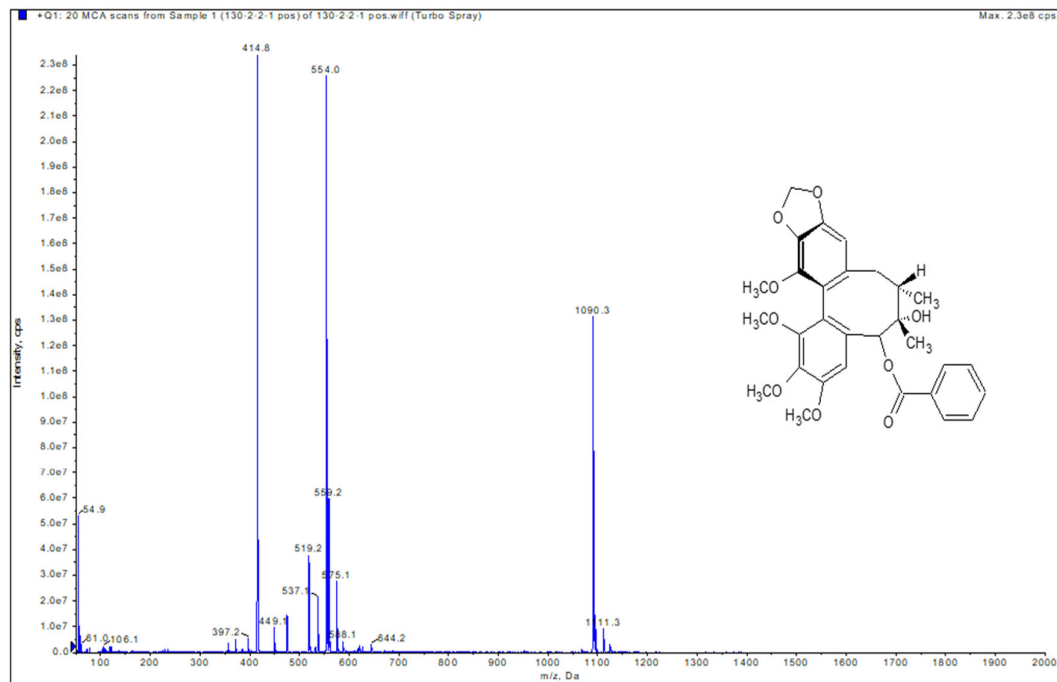


Figure S34. LR-MS chromatogram of compound 4

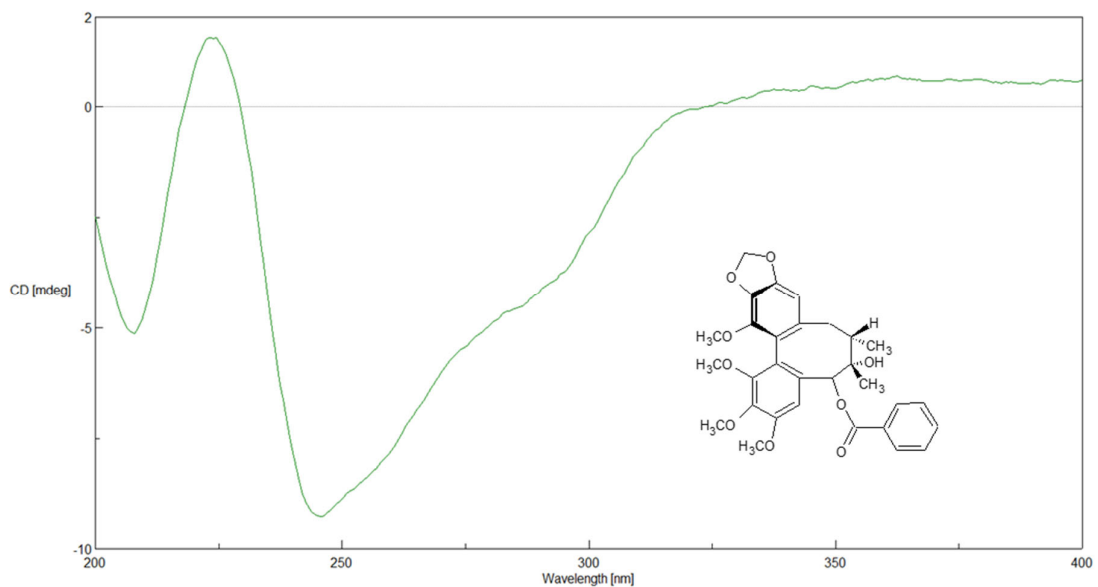


Figure S35. CD spectrum of compound 4 in methanol ($c = 1 \text{ mg/mL}$)

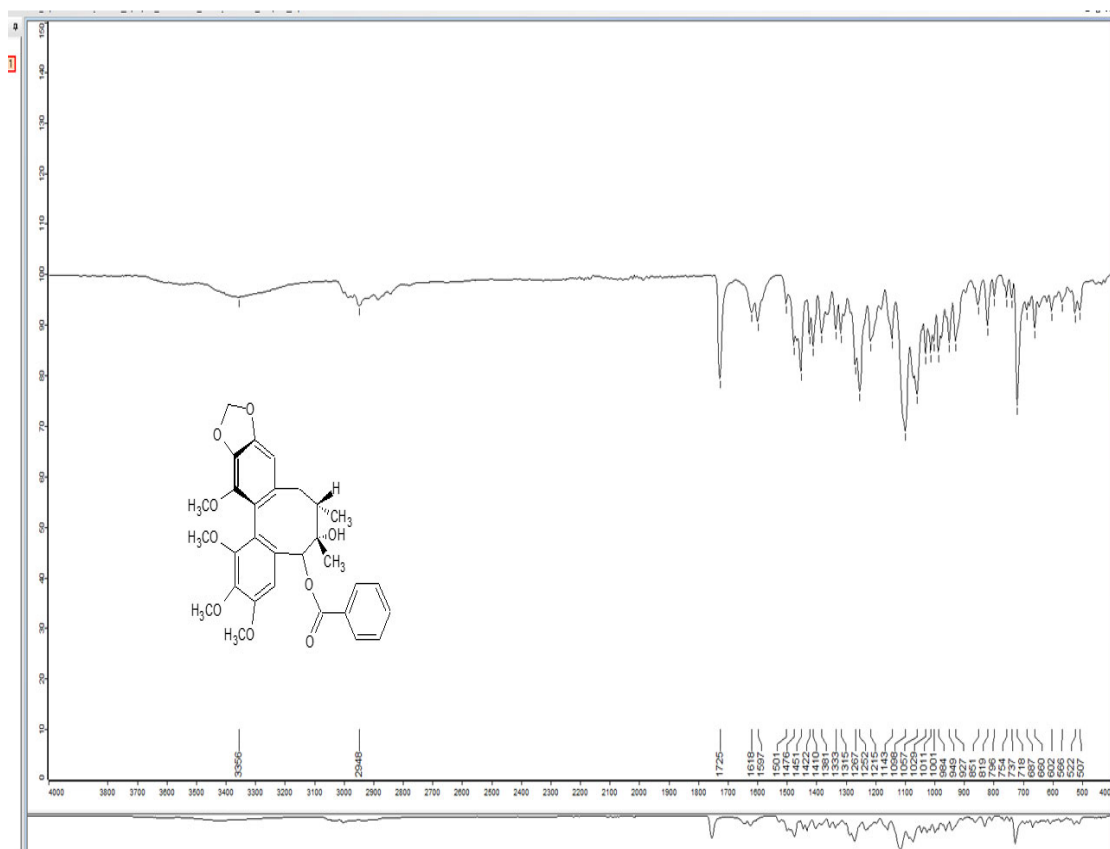


Figure S36. IR spectrum of compound 4

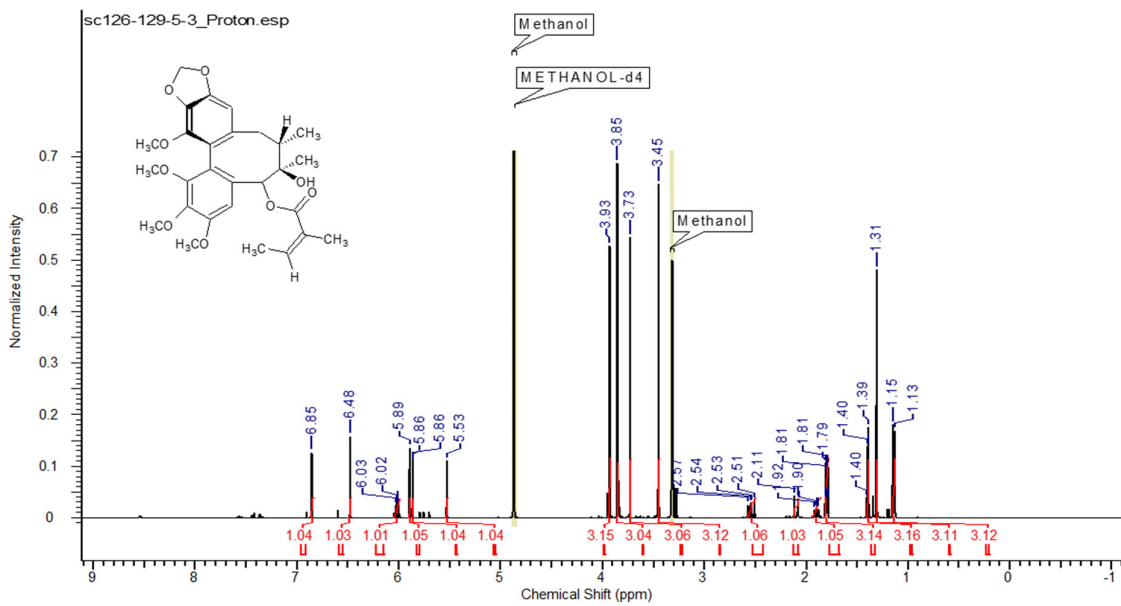


Figure S37. ^1H NMR spectrum of compound 5 in CD_3OD

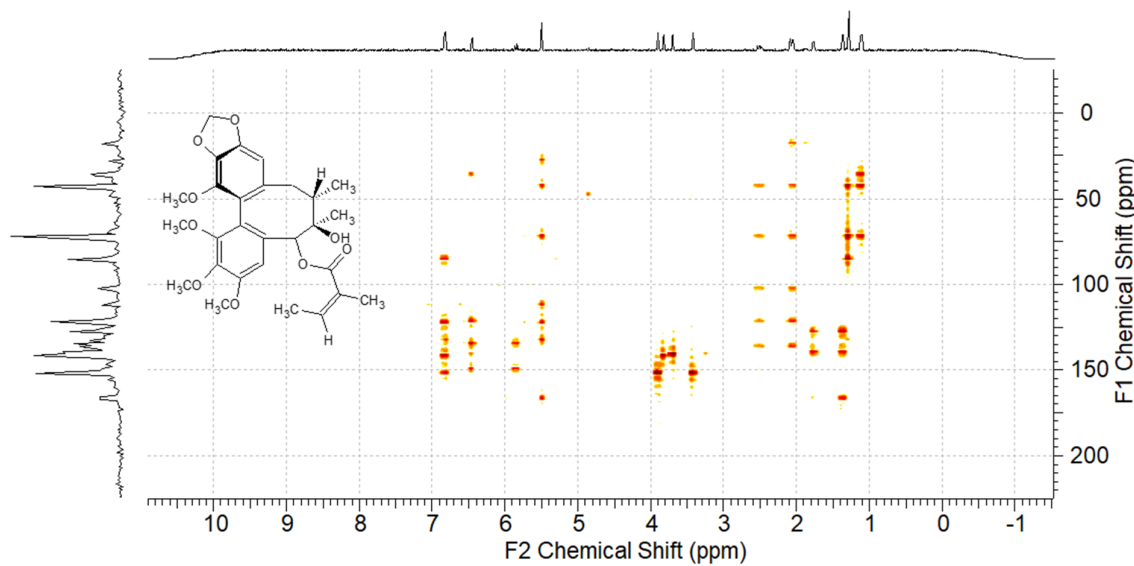


Figure S38. HMBC NMR spectrum of compound 5 in CD_3OD

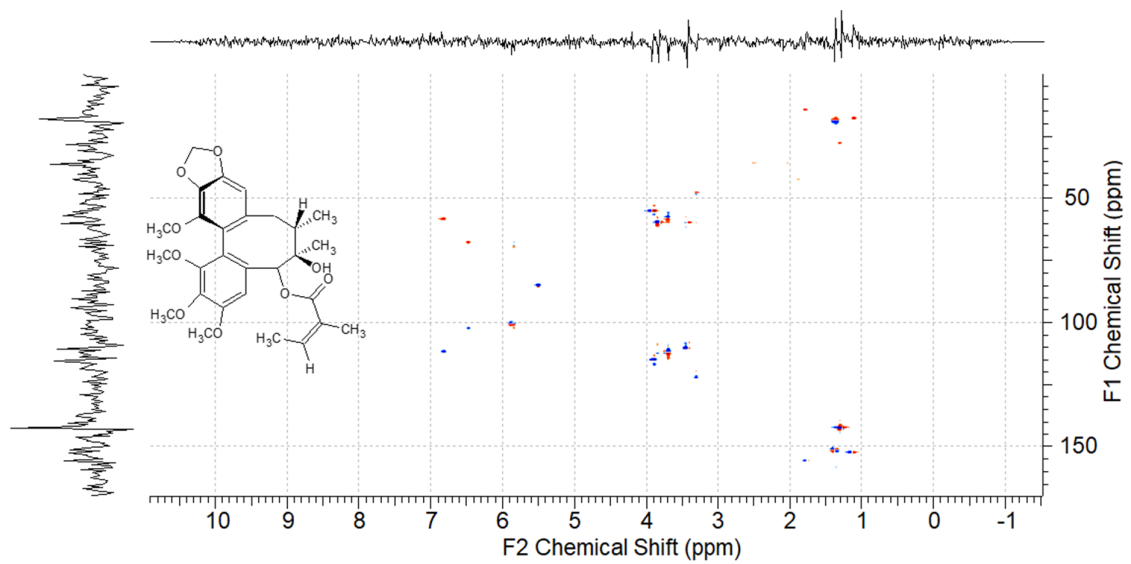


Figure S39. HSQC NMR spectrum of compound 5 in CD_3OD

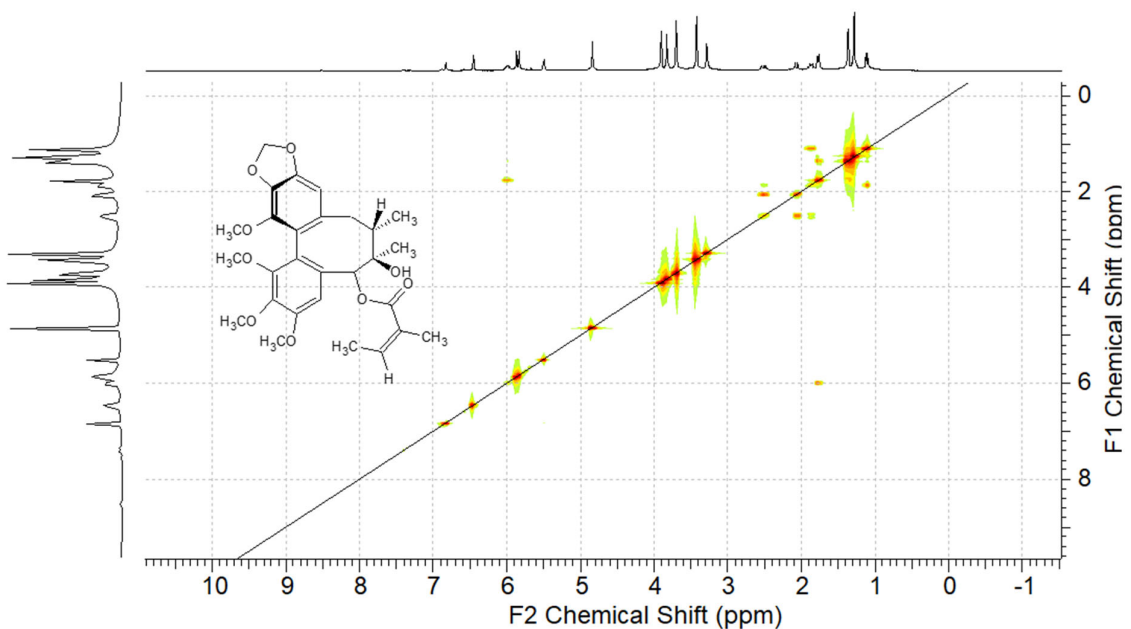


Figure S40. COSY NMR spectrum of compound 5 in CD_3OD

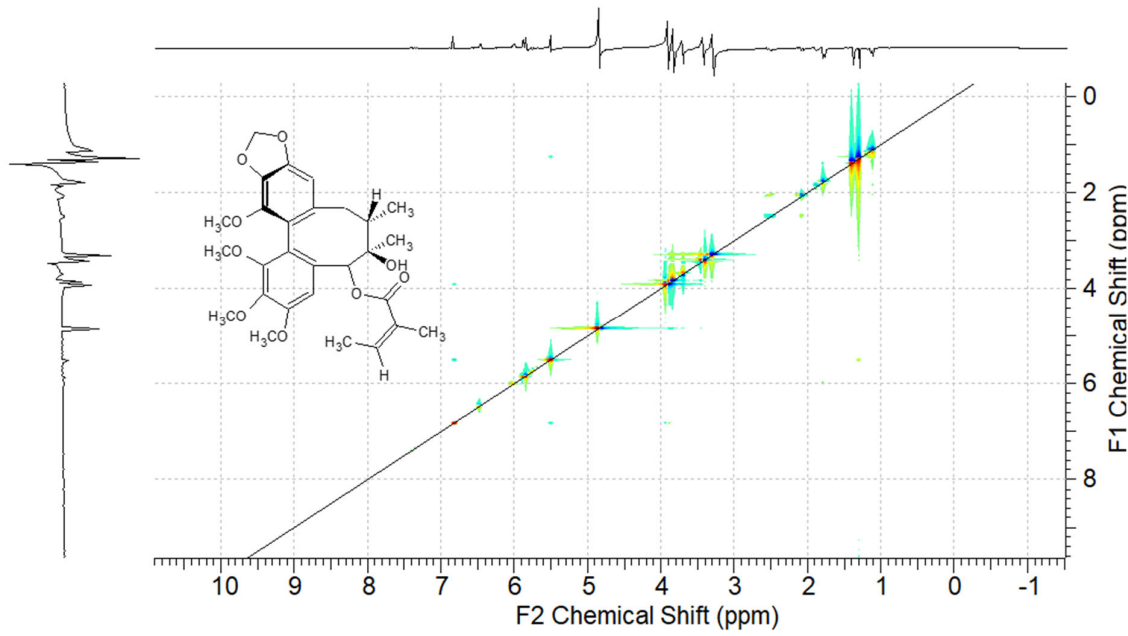


Figure S41. NOESY NMR spectrum of compound 5 in CD_3OD

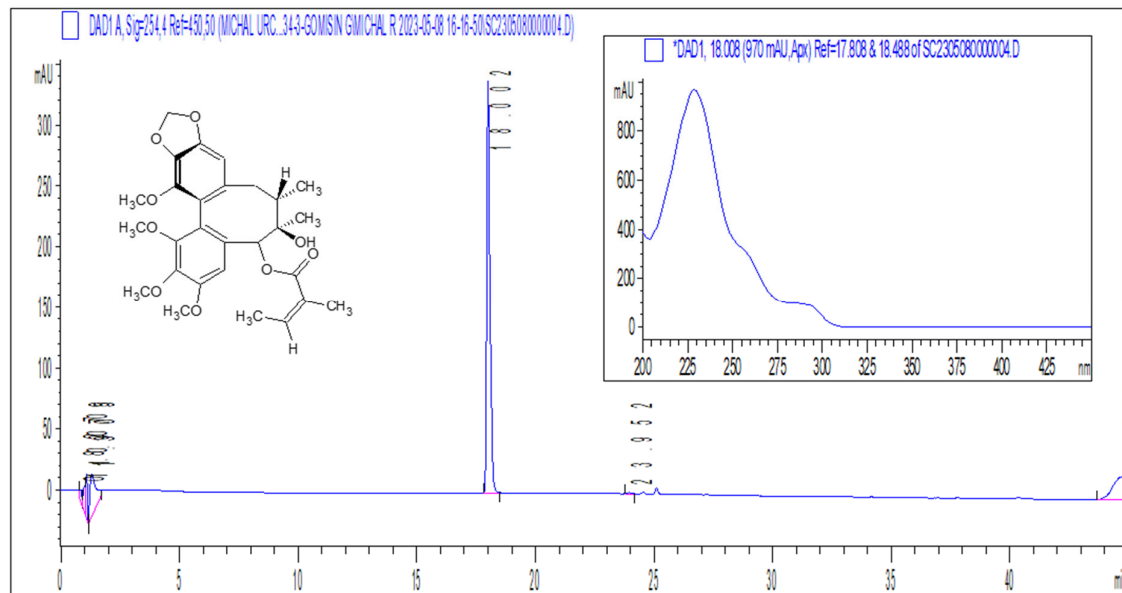


Figure S42. HPLC-DAD chromatogram of compound 5

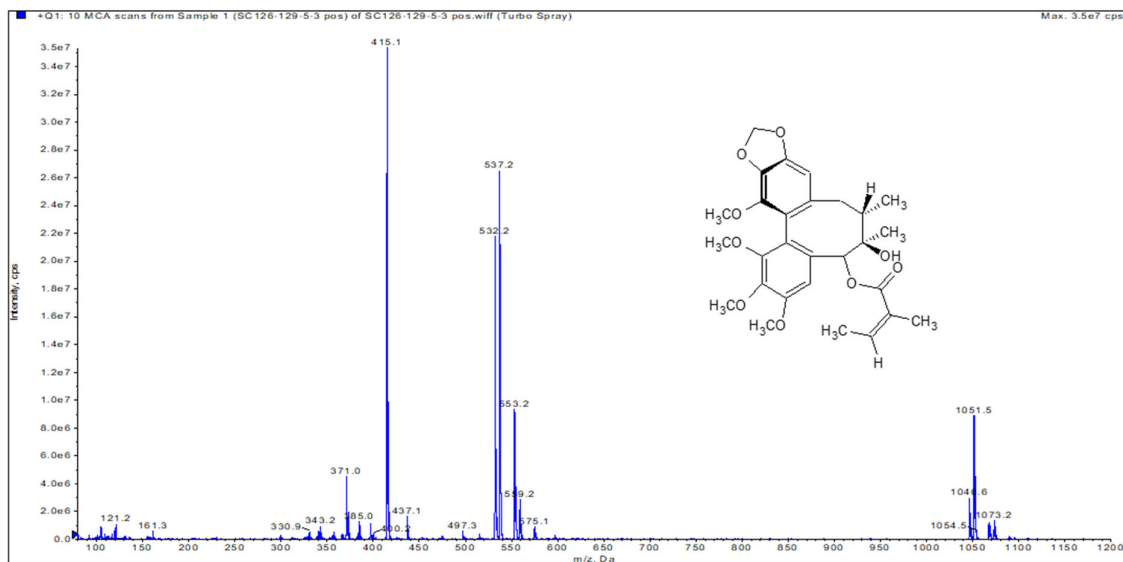


Figure S43. LR-MS spectrum of compound 5

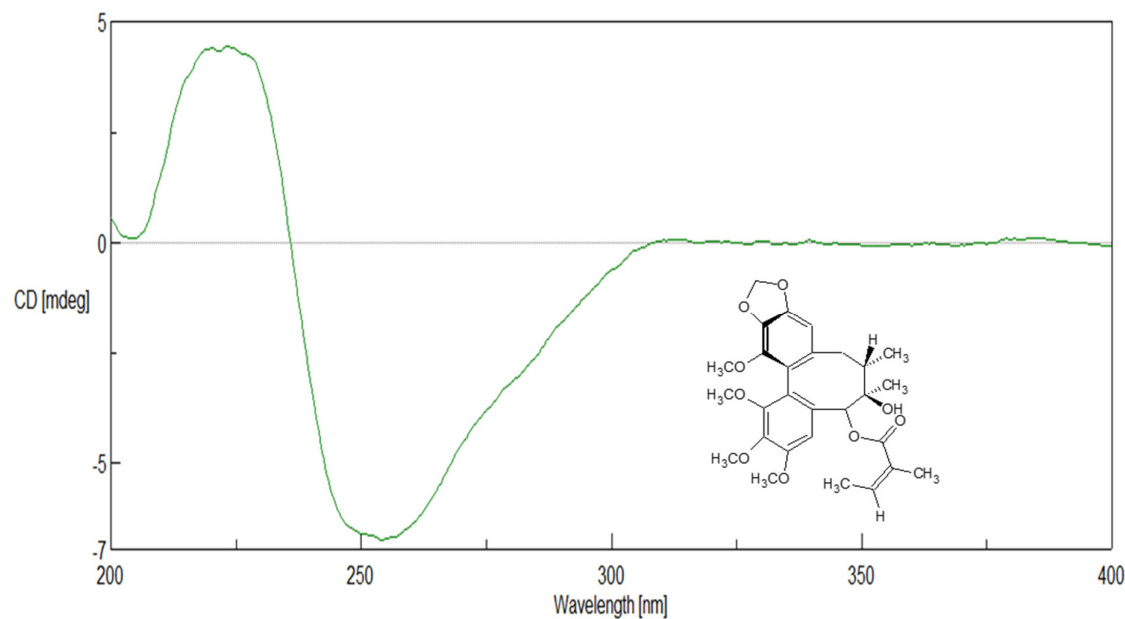


Figure S44. CD spectrum of compound 5 in methanol (c=1 mg/mL)

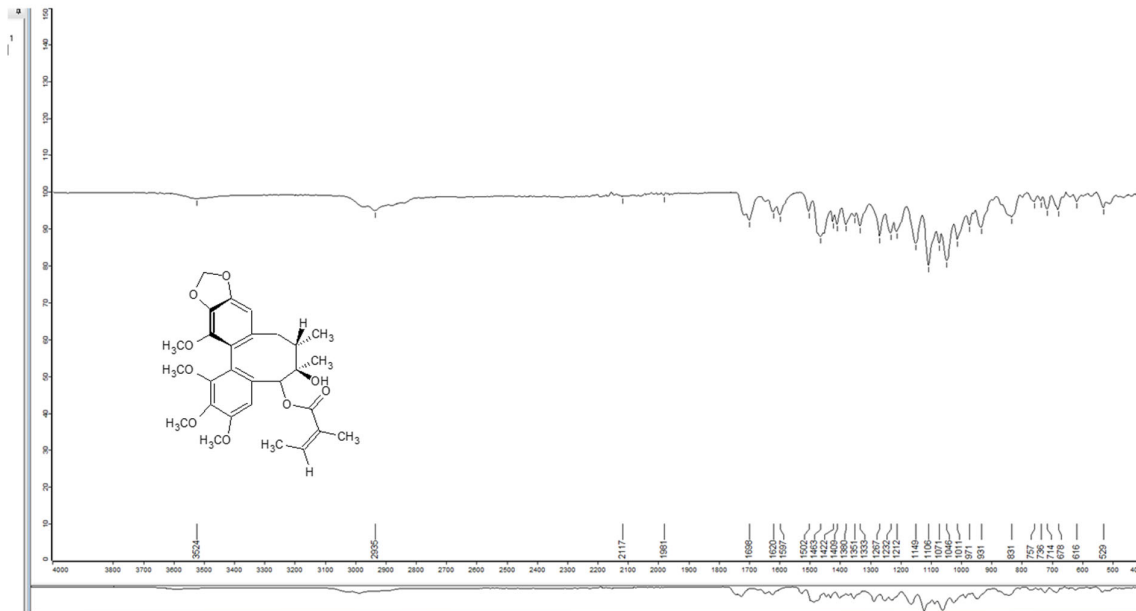


Figure S45. IR spectrum of compound 5

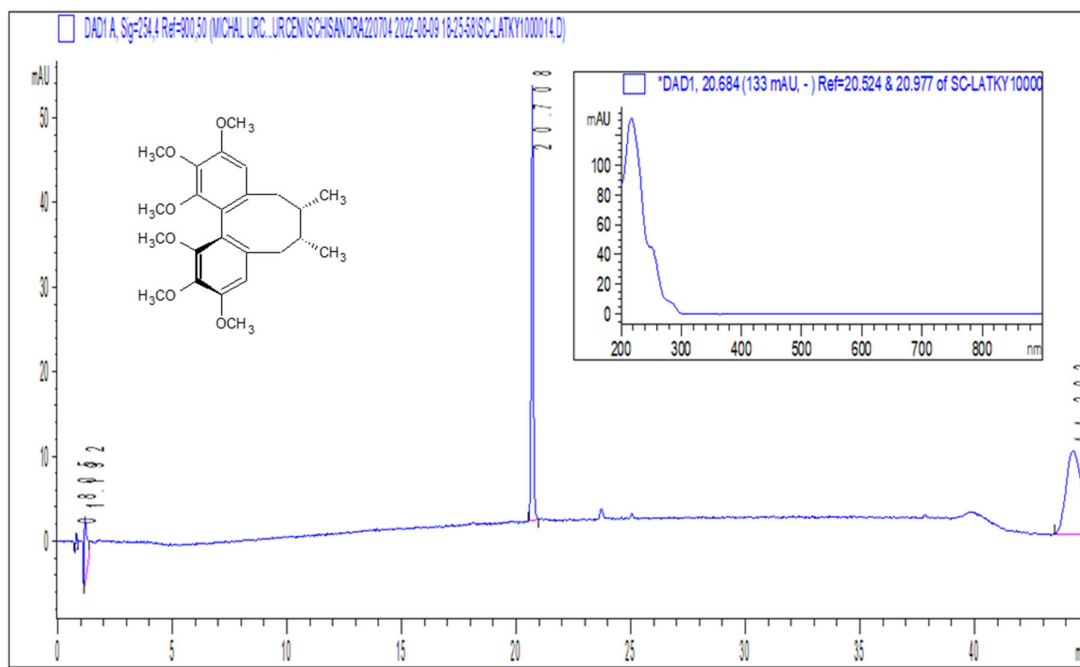


Figure S46. HPLC-DAD chromatogram of common injection of compound 6 with standard of (+)-deoxyschisandrin; UV spectrum of peak corresponding to (+)-deoxyschisandrin.

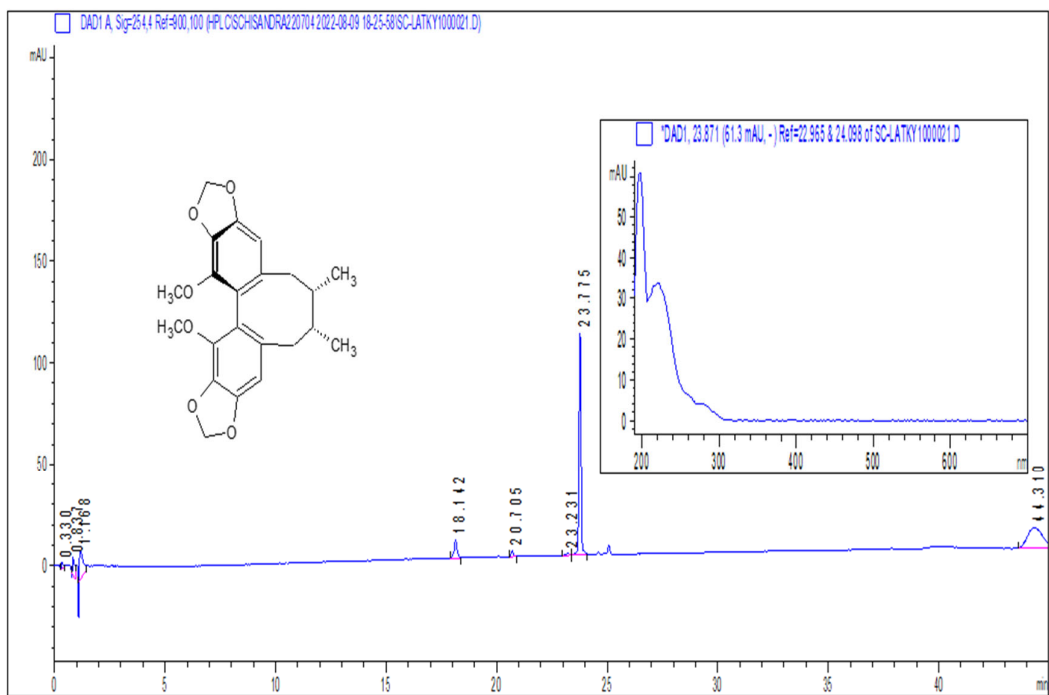


Figure S47. HPLC-DAD chromatogram of common injection of (-)-wuweizisu C with standard of (-)-wuweizisu C; UV spectrum of peak corresponding to (-)-wuweizisu C.

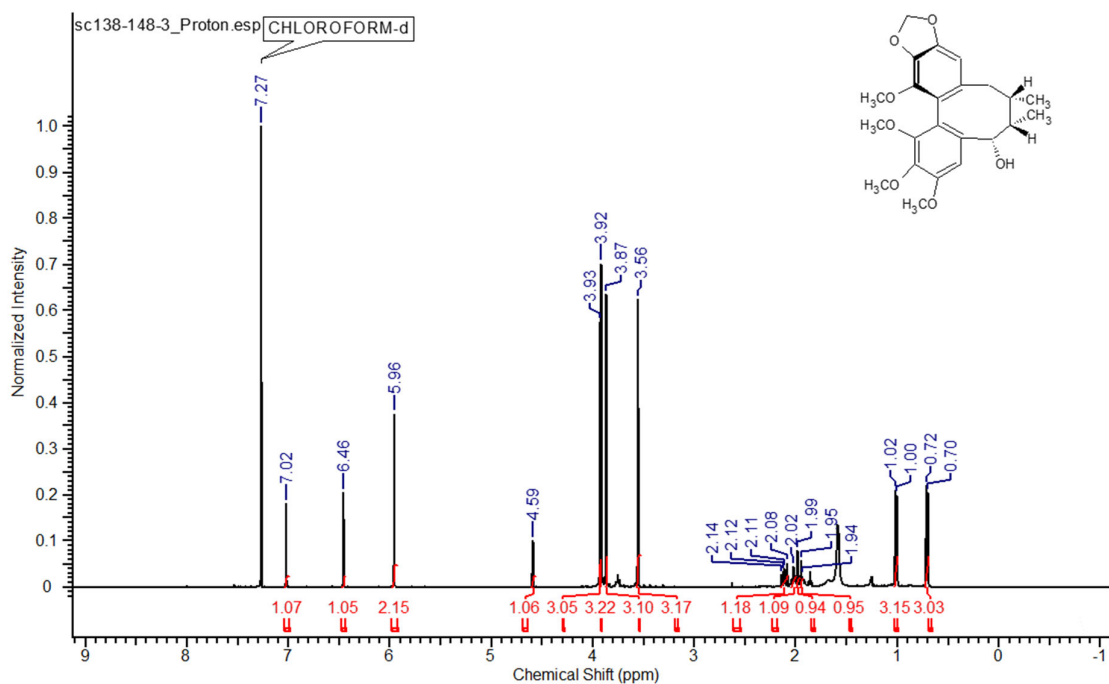


Figure S48. ^1H NMR spectrum of epigomisin O in CDCl_3

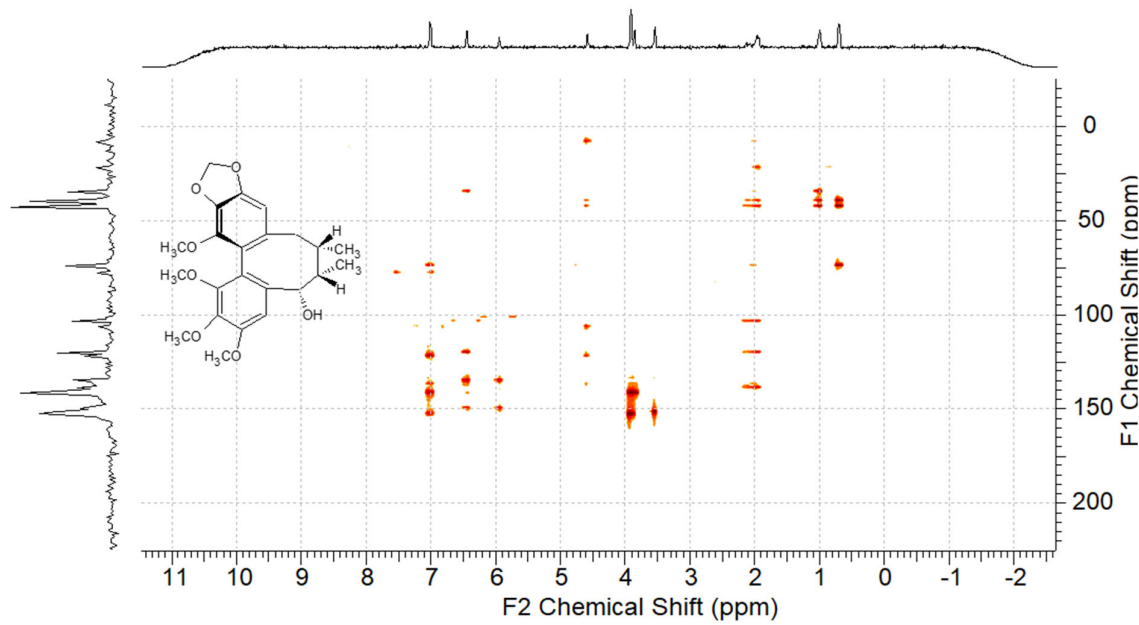


Figure S49. HMBC NMR spectrum of epigomisin O in CDCl_3

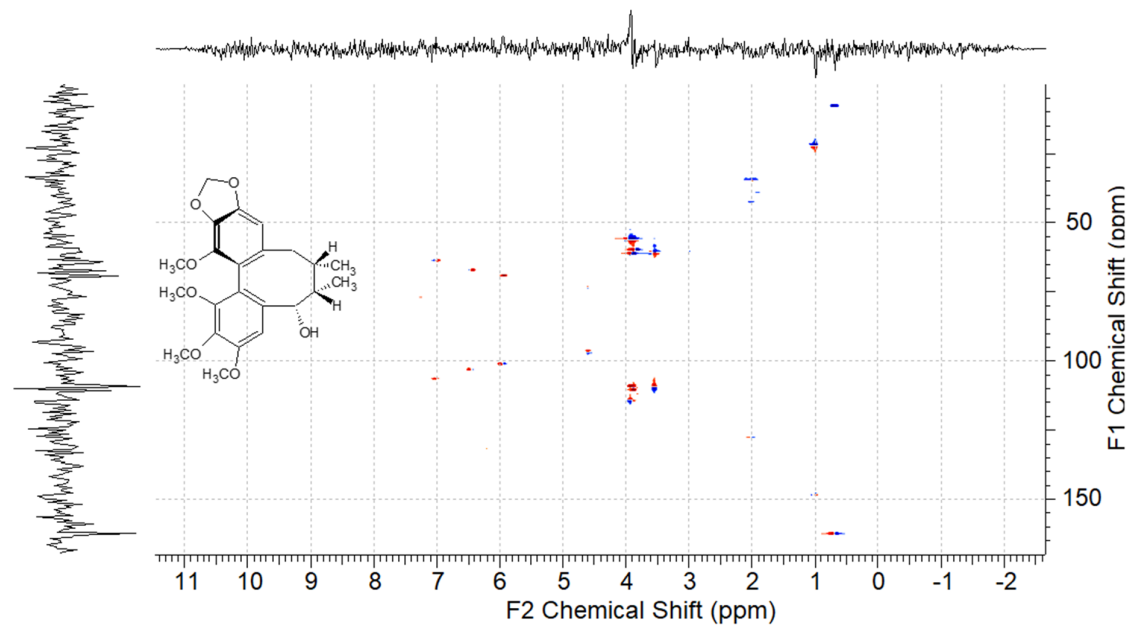


Figure S50. HSQC NMR spectrum of epigomisin O in CDCl_3

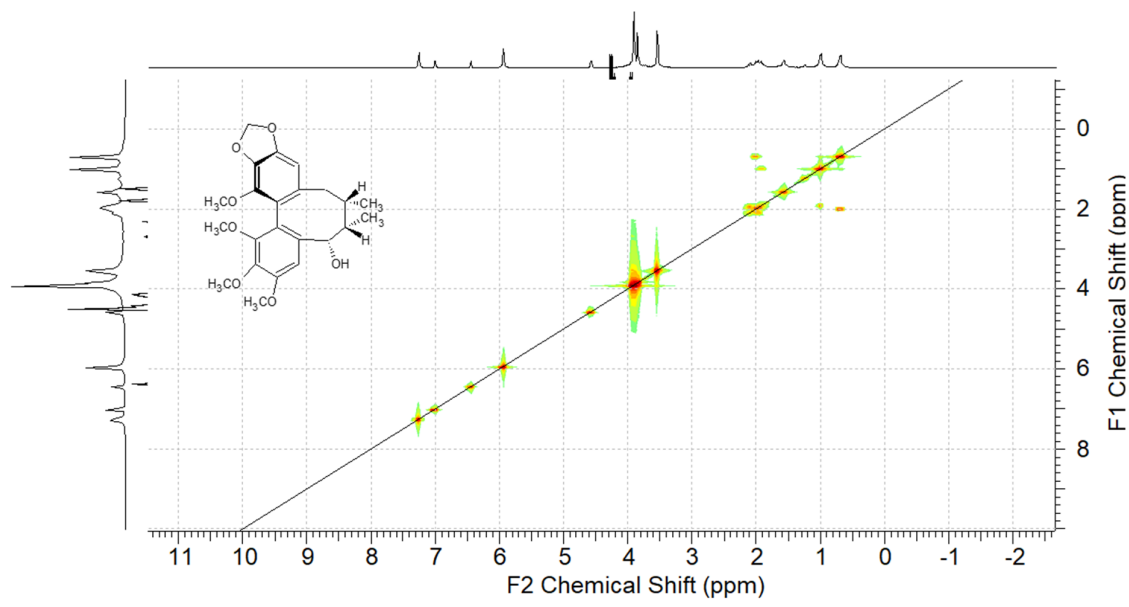


Figure S51. COSY NMR spectrum of epigomisin O in CDCl_3

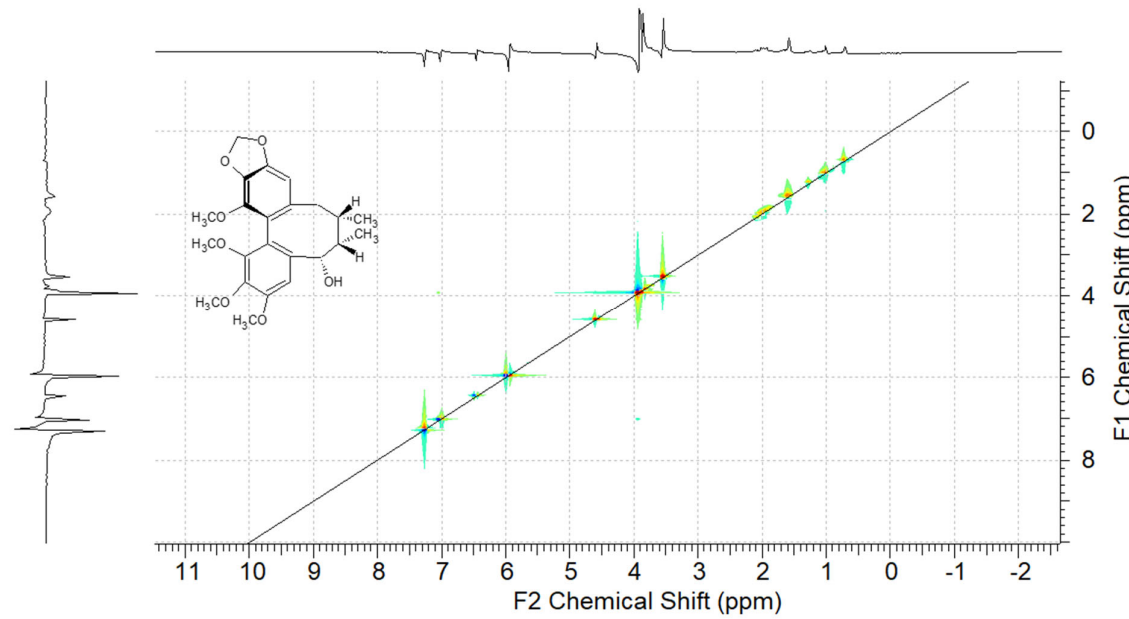


Figure S52. NOESY NMR spectrum of epigomisin O in CDCl_3

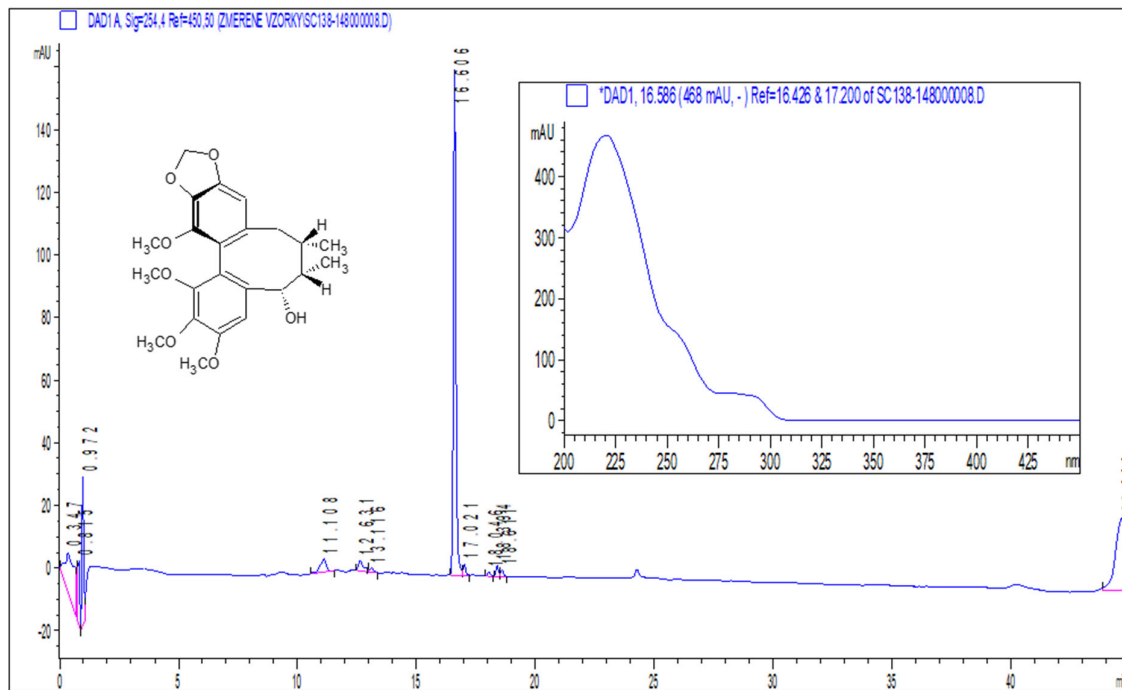


Figure S53. HPLC-DAD chromatogram of epigomisin O

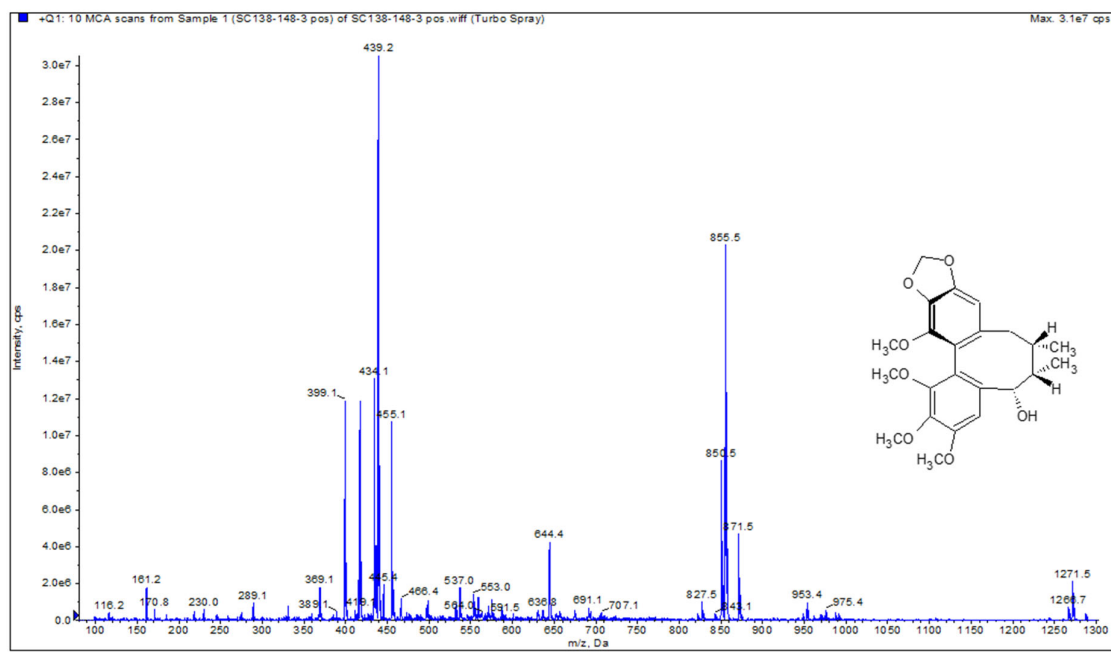


Figure S54. LR-MS spectrum of epigomisin O

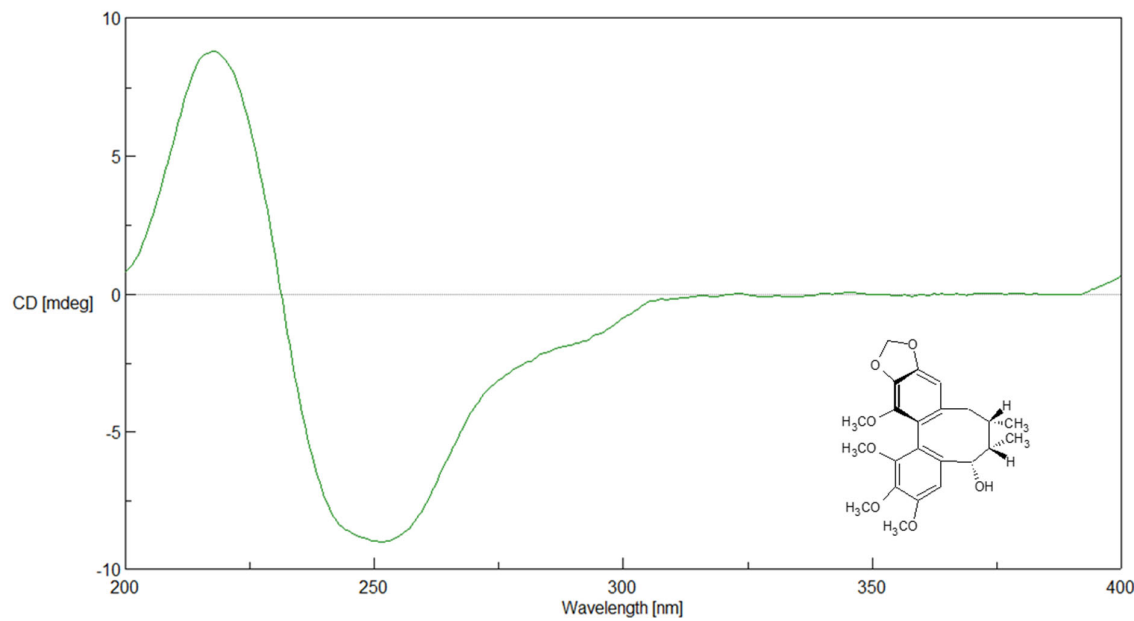


Figure S55. CD spectrum of epigomisin O in methanol ($c=1$ mg/mL)

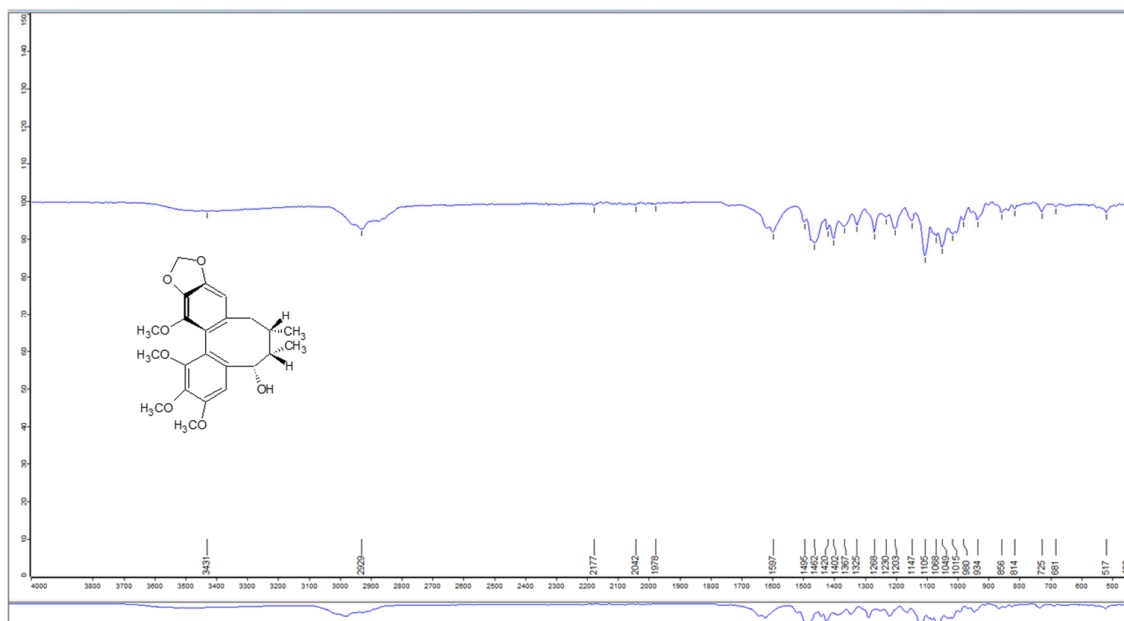


Figure S56. IR spectrum of epigomisin O

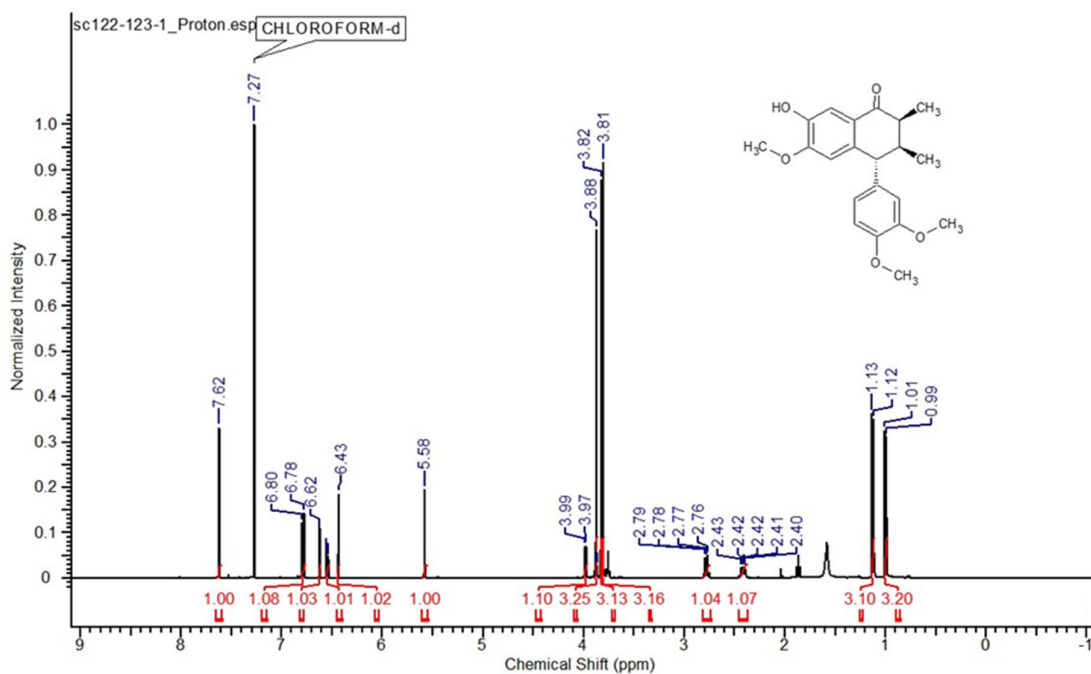


Figure S57. ^1H NMR spectrum of arisantetralone C in CDCl_3

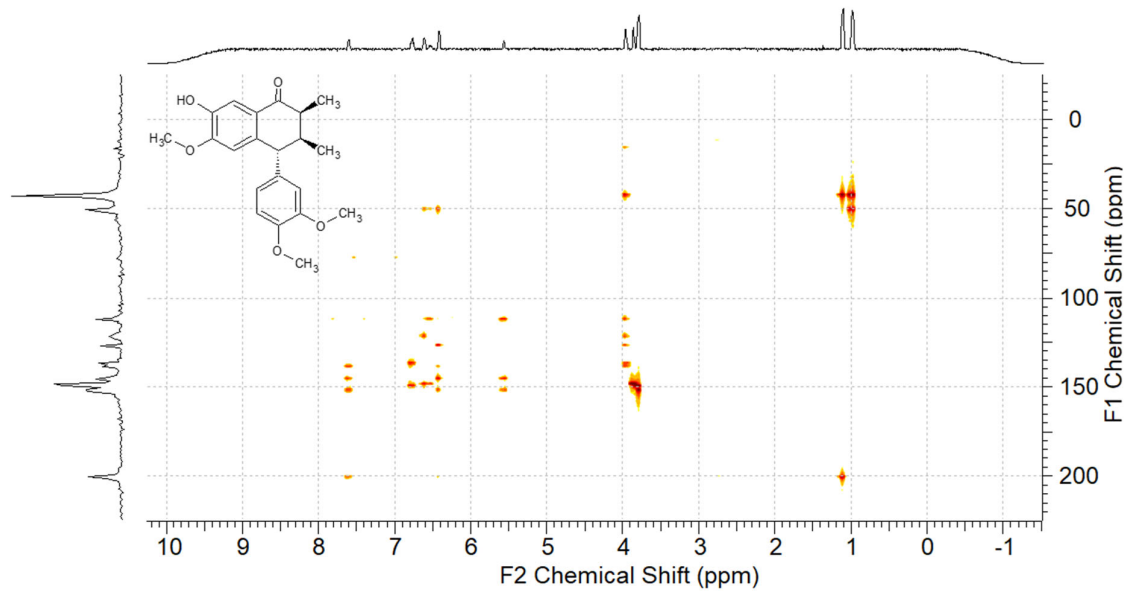


Figure S58. HMBC NMR spectrum of arisantetralone C in CDCl_3

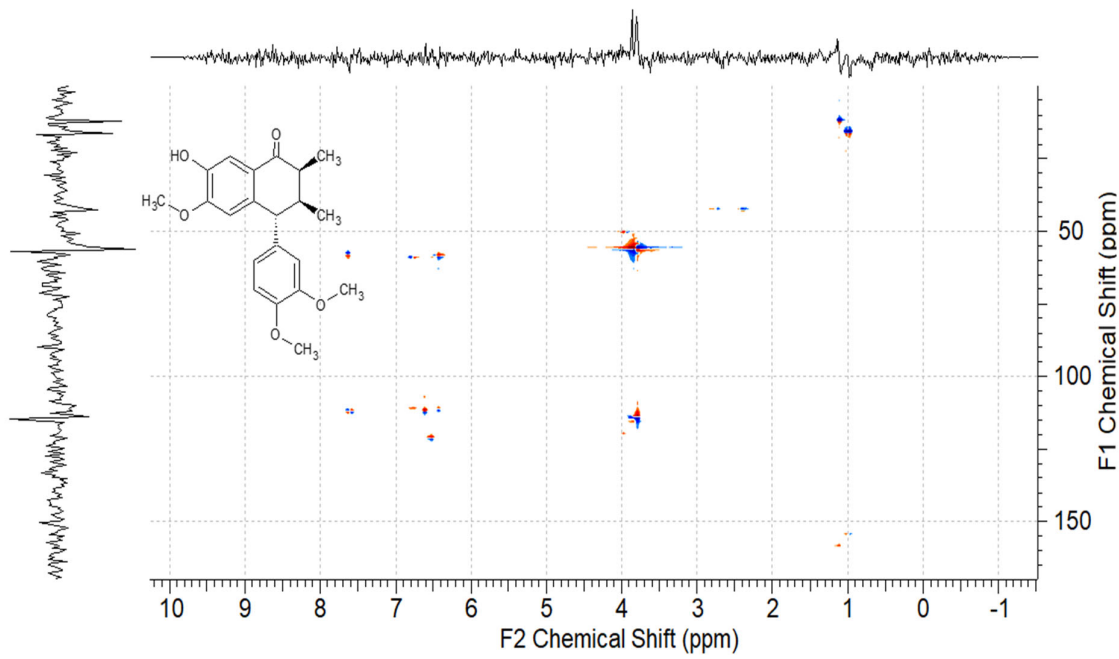


Figure S59. HSQC NMR spectrum of arisantetralone C in CDCl_3

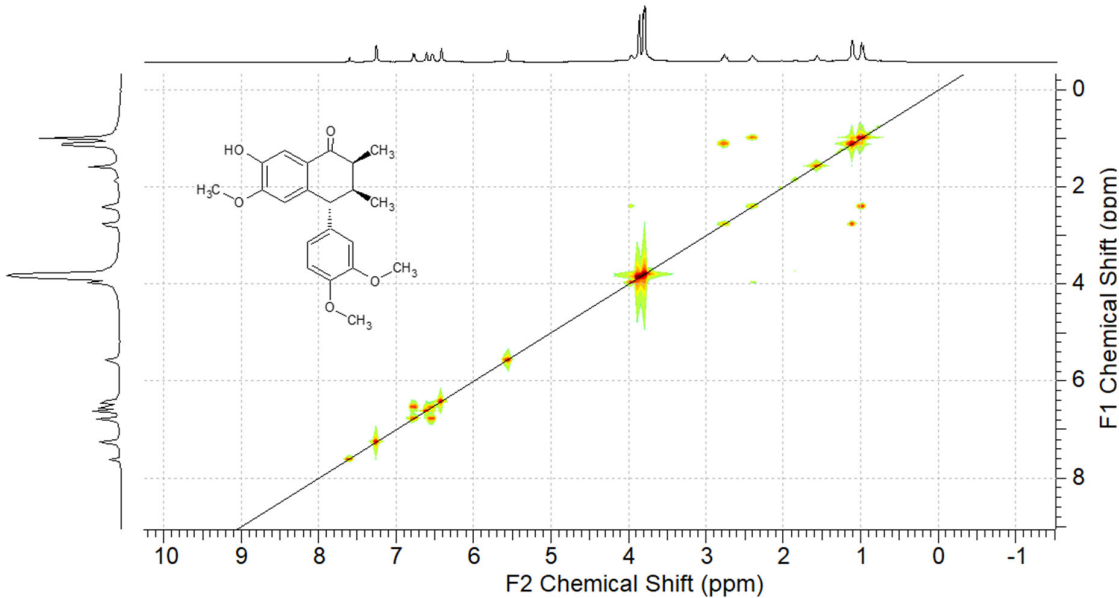


Figure S60. COSY NMR spectrum of arisantetralone C in CDCl_3

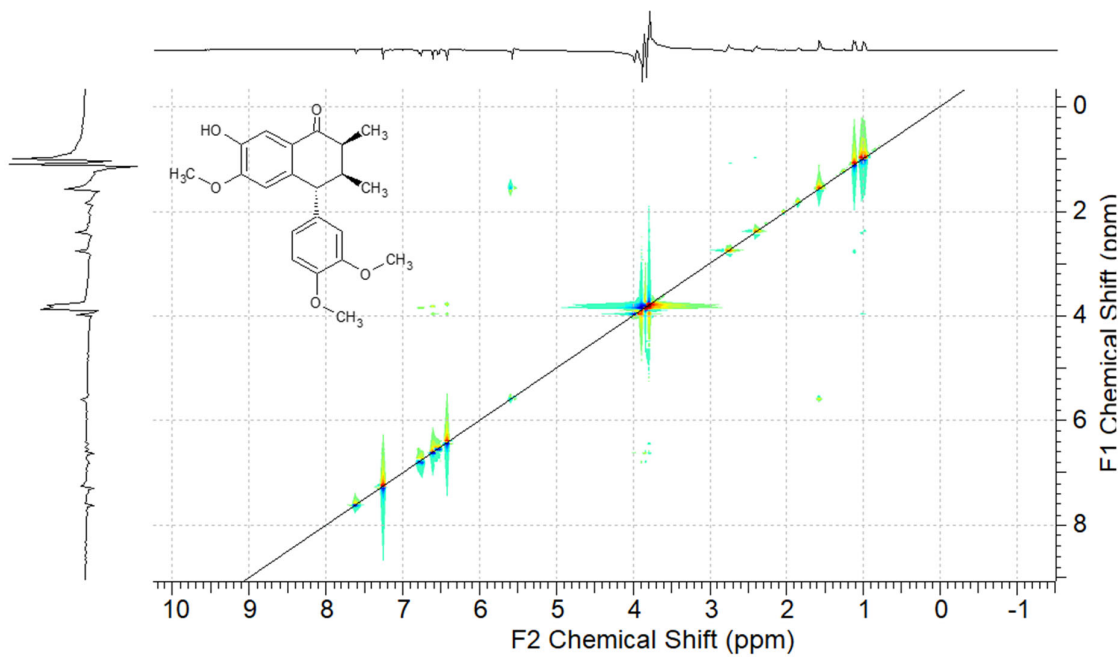


Figure S61. NOESY NMR spectrum of arisantetralone C in CDCl_3

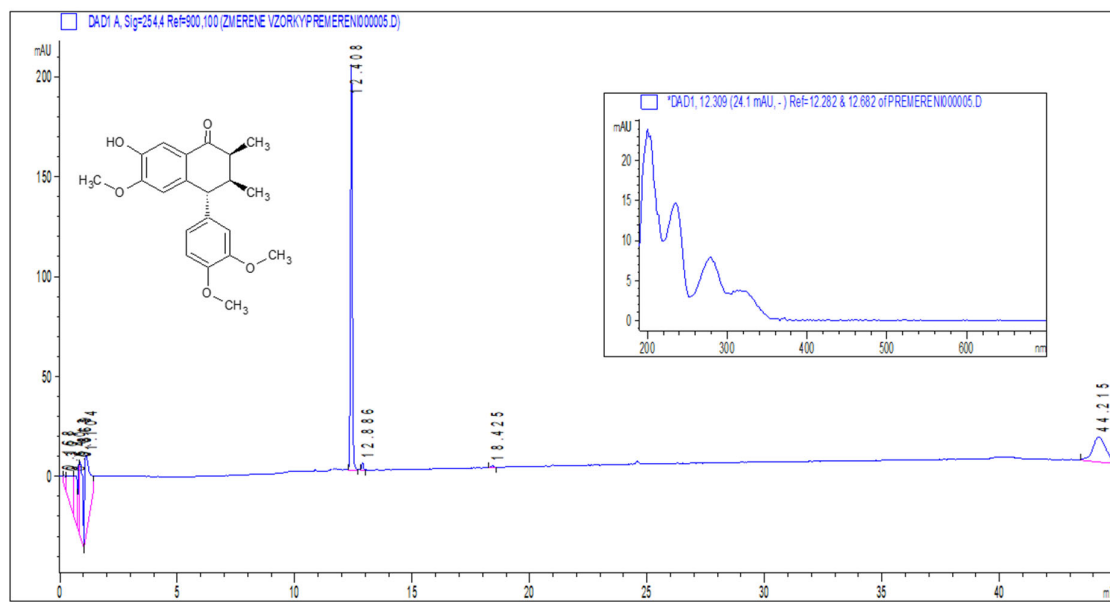


Figure S62. HPLC-DAD chromatogram of arisantetralone C

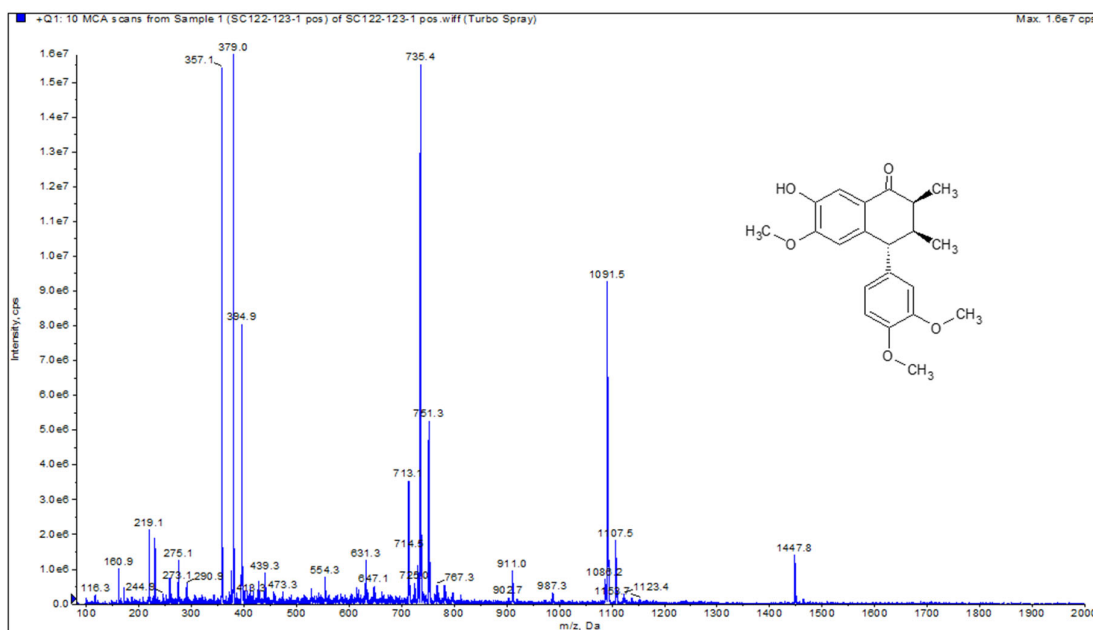


Figure S63. LR-MS spectrum of arisantetralone C

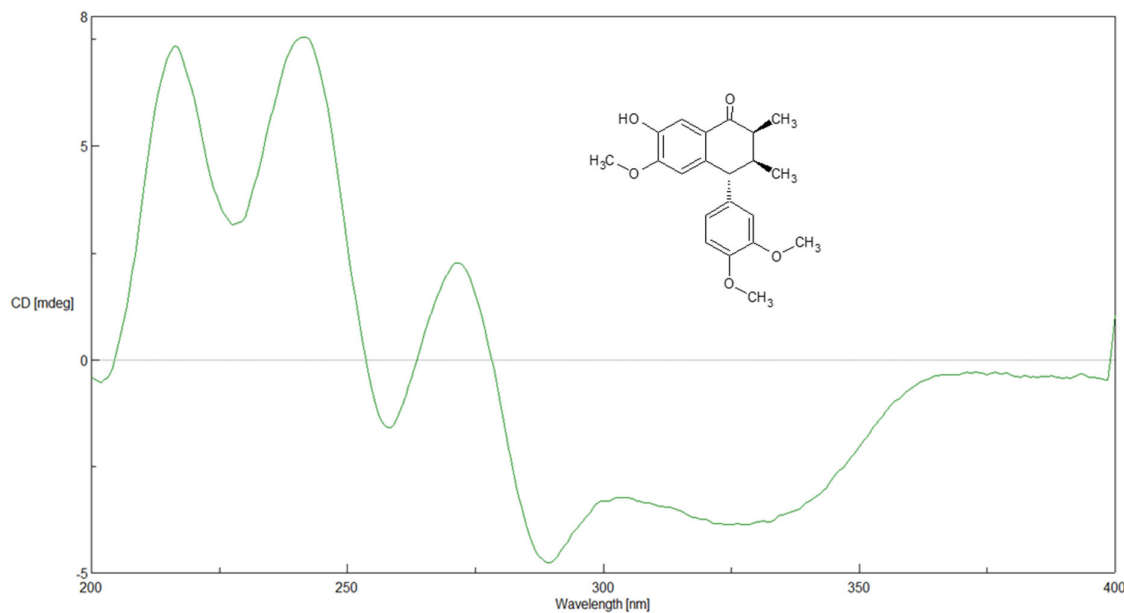


Figure S64. CD spectrum of arisantetralone C in methanol (c = 1 mg/mL)

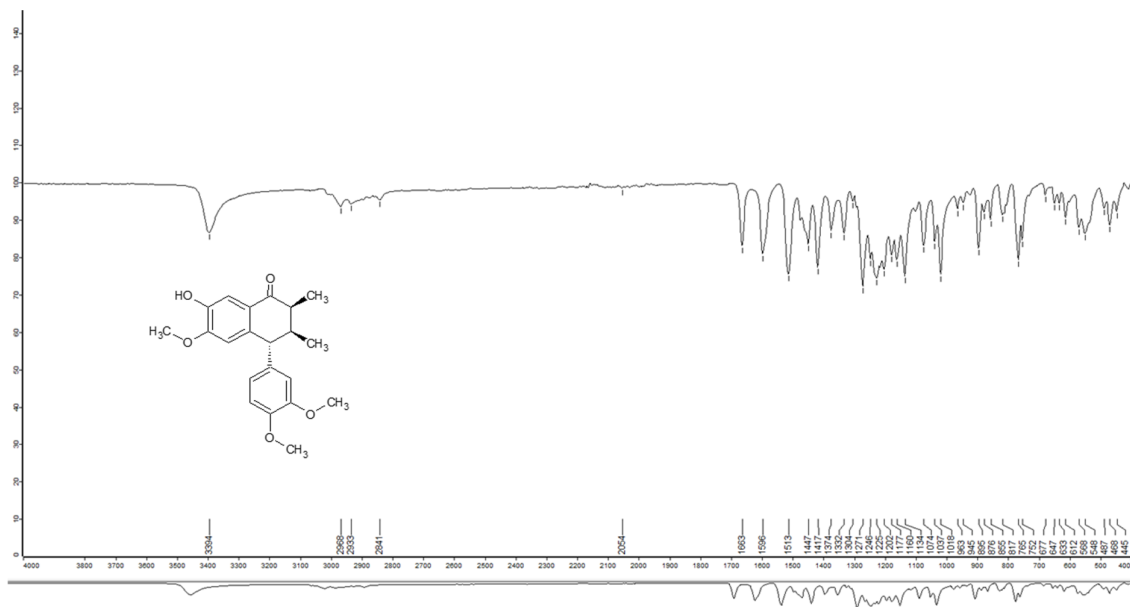


Figure S65. IR spectrum of arisantetralone C

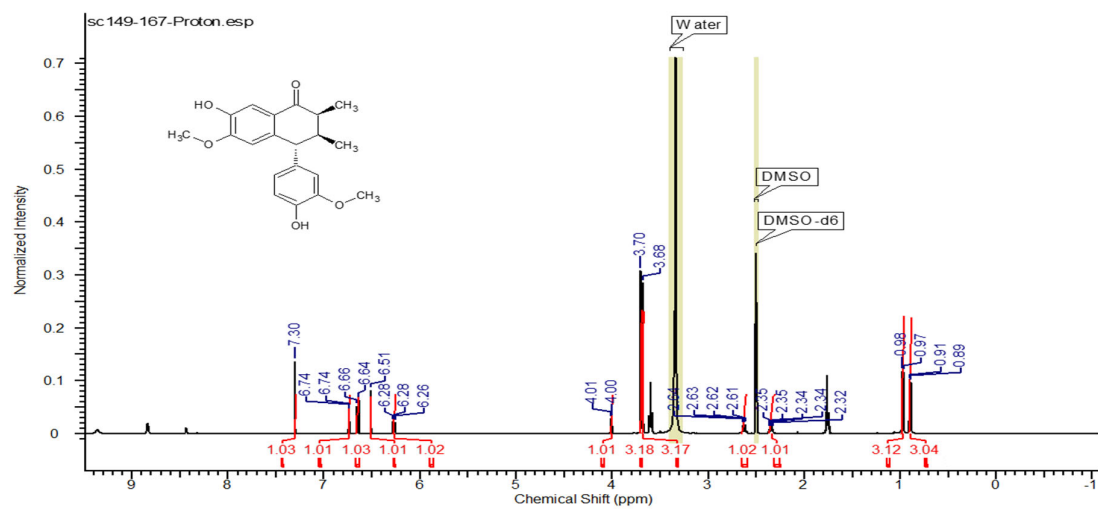


Figure S66. ¹H NMR spectrum of arisantetralone A in DMSO-*d*₆

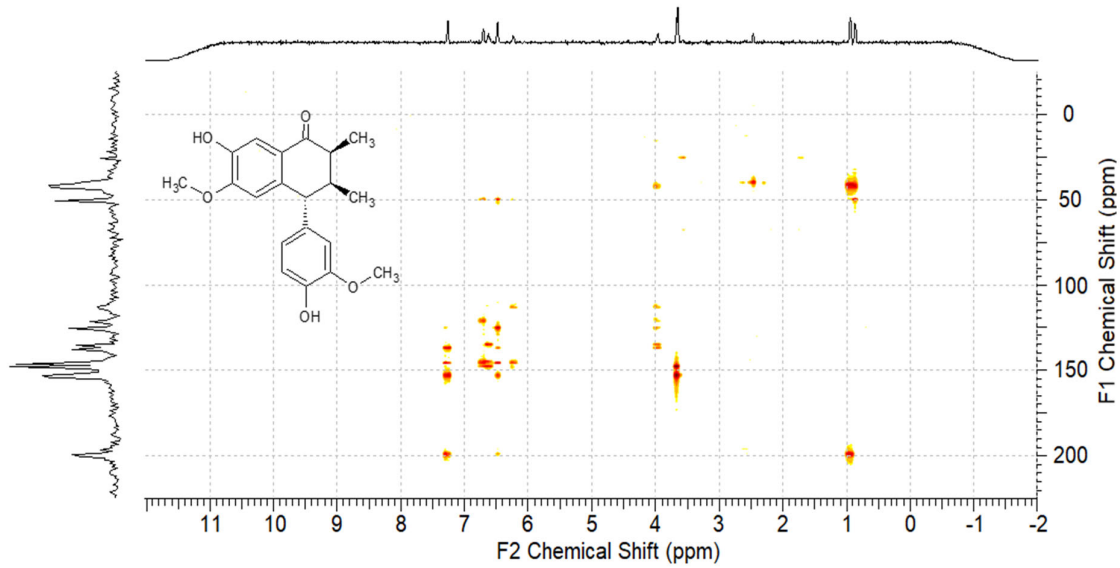


Figure S67. HMBC NMR spectrum of arisantetralone A in $\text{DMSO}-d_6$

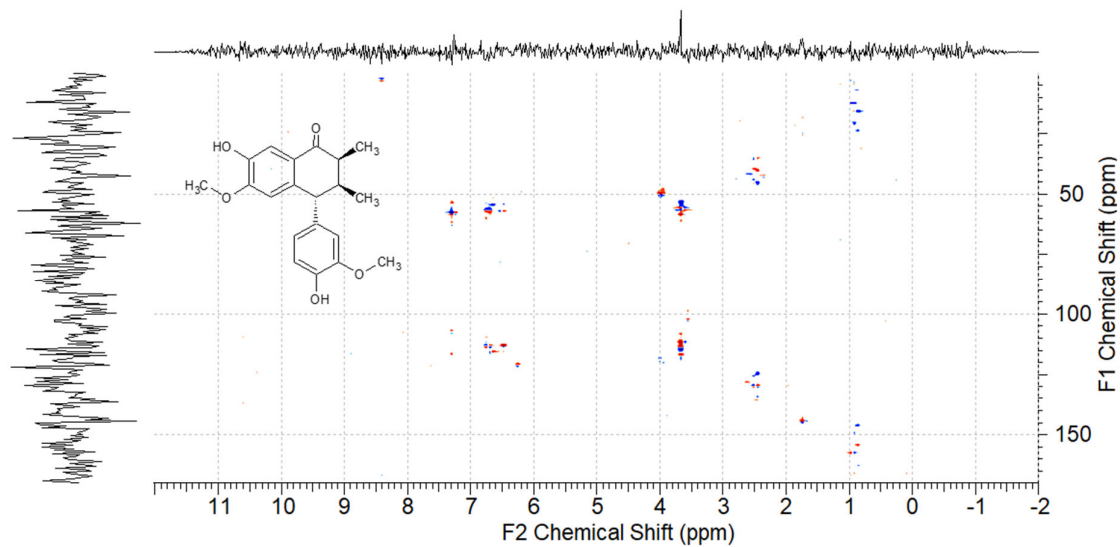


Figure S68. HSQC NMR spectrum of arisantetralone A in $\text{DMSO}-d_6$

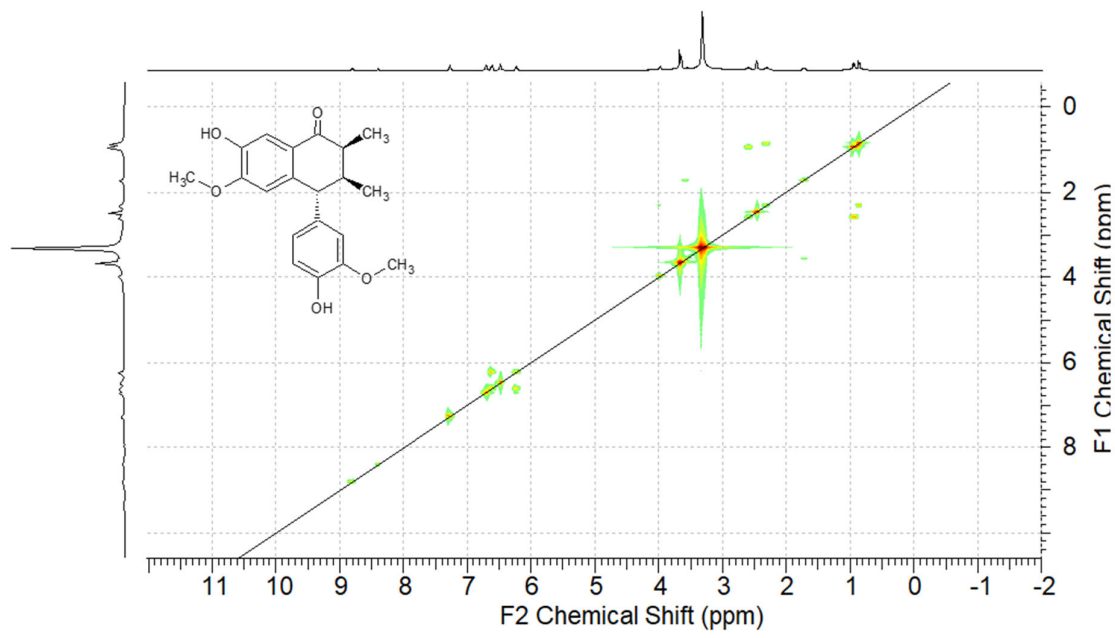


Figure 69. COSY NMR spectrum of arisantetralone A in $\text{DMSO}-d_6$

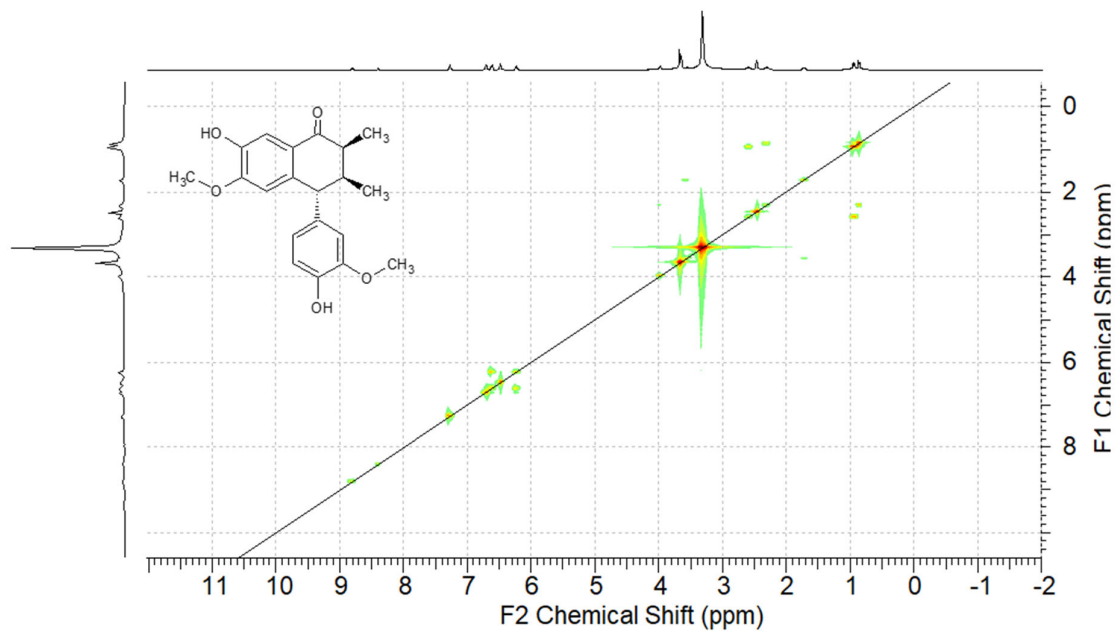


Figure S70. NOESY NMR spectrum of arisantetralone A in $\text{DMSO}-d_6$

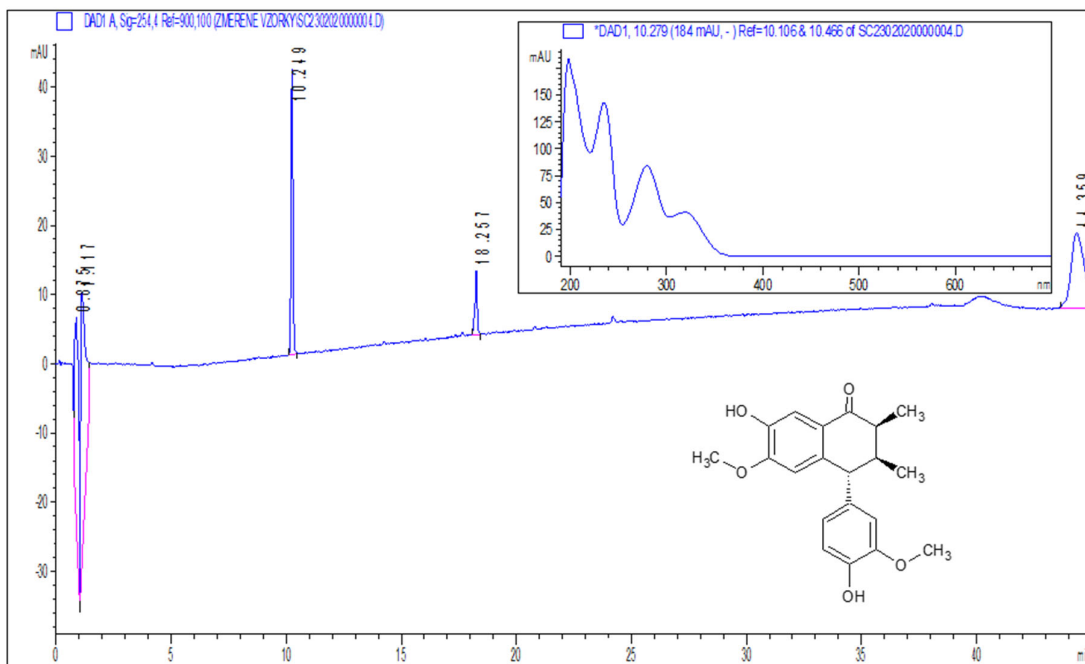


Figure S71. HPLC-DAD chromatogram of arisantetralone A

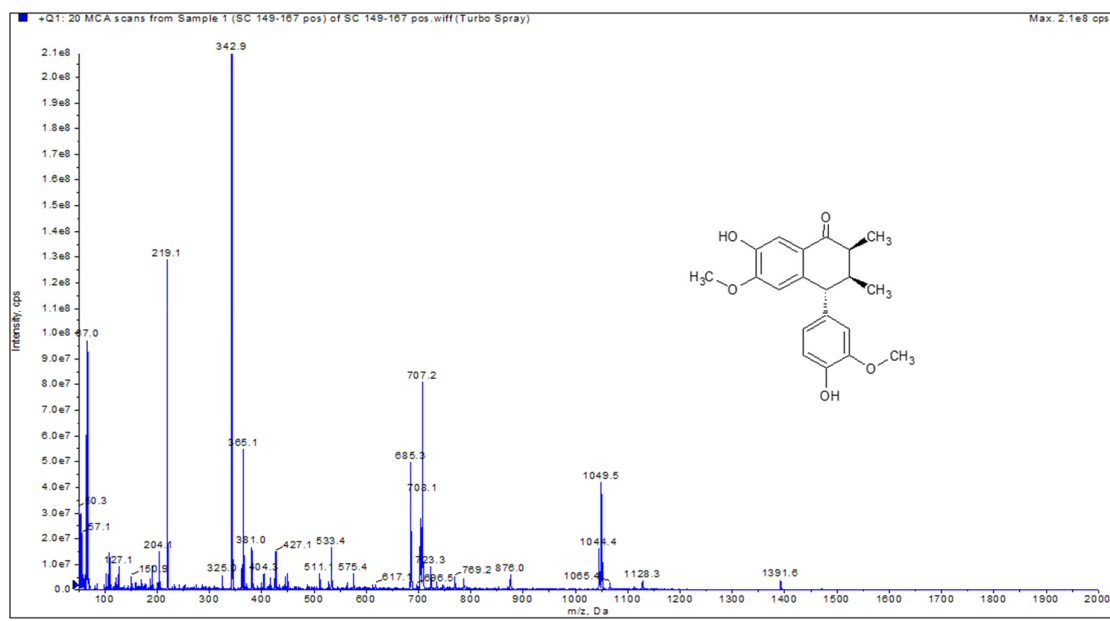


Figure S72. LR-MS spectrum of arisantetralone A

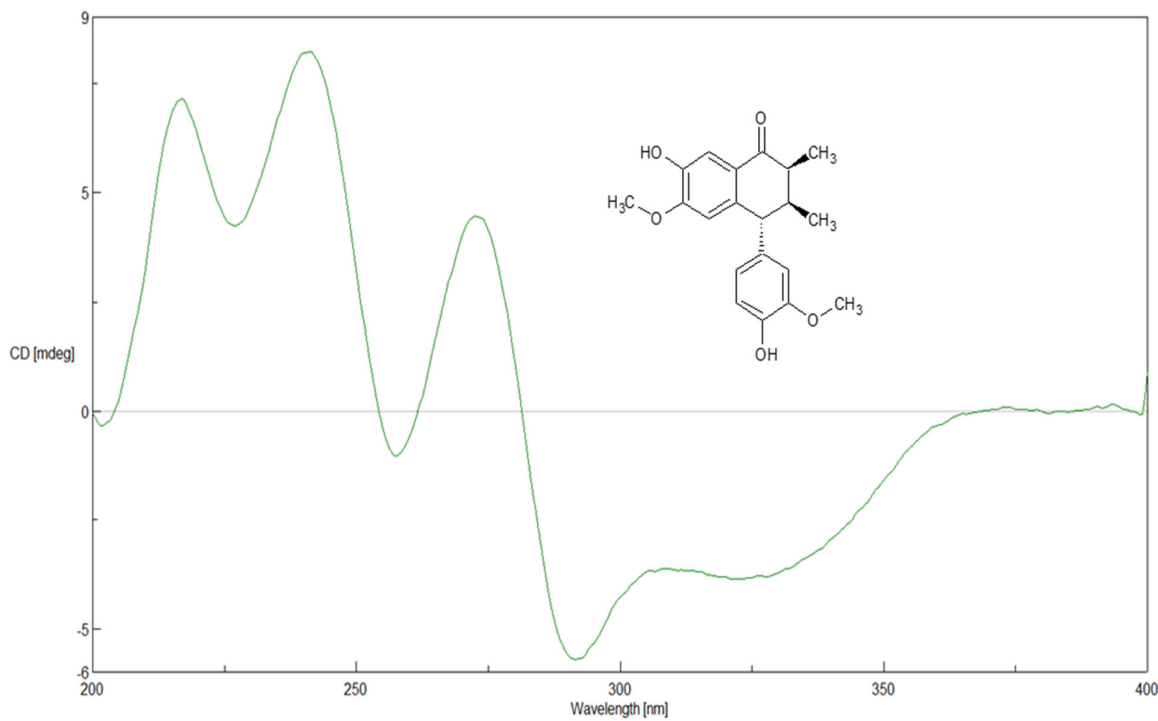


Figure S73. CD spectrum of arisantetralone A in methanol ($c=1$ mg/mL)

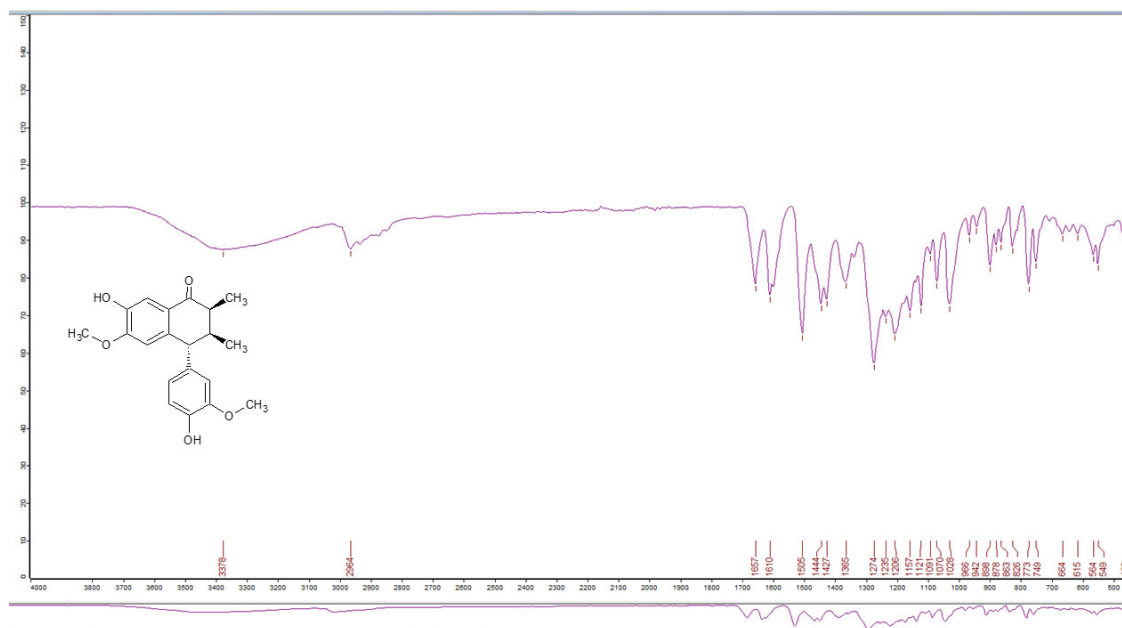


Figure S74. IR spectrum of arisantetralone A

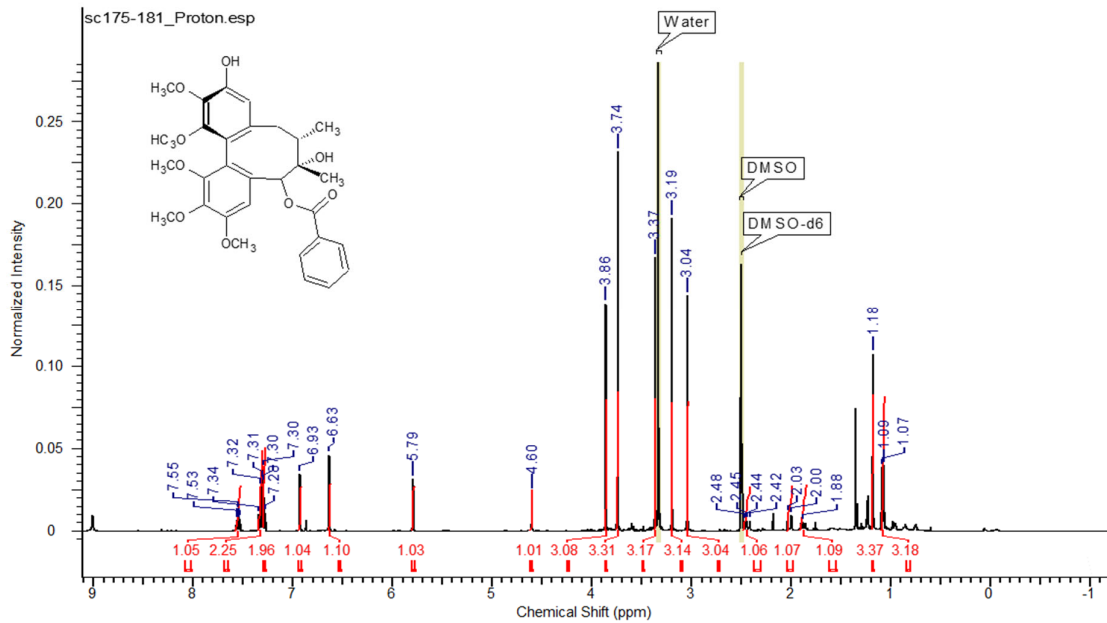


Figure S75. ^1H NMR spectrum of (-)-schisantherin E in $\text{DMSO}-d_6$

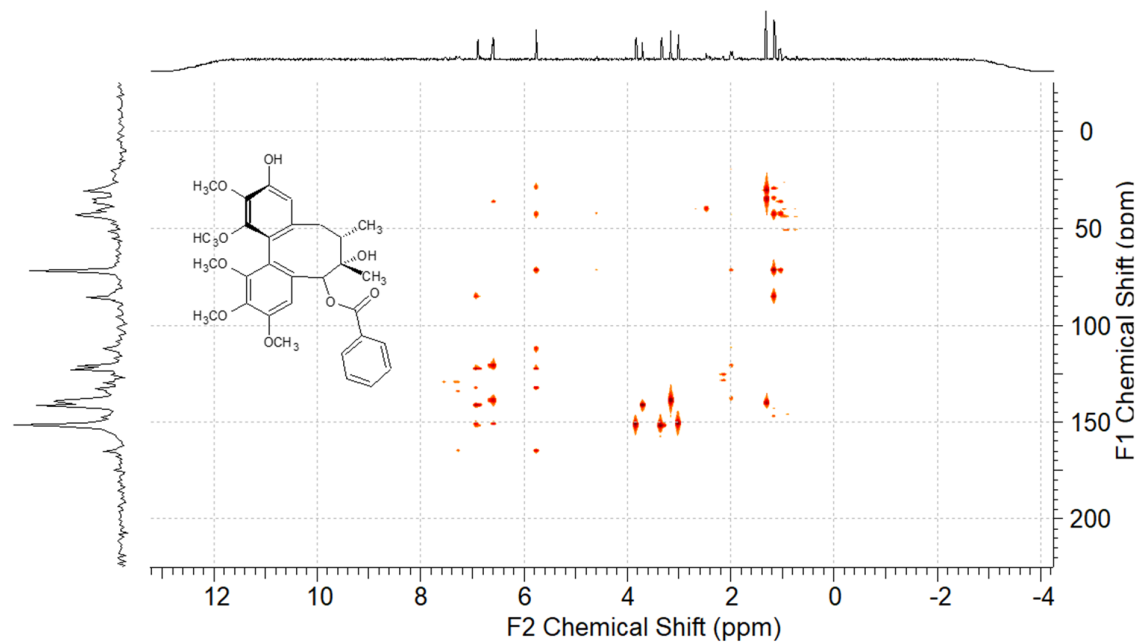


Figure S76. HMBC NMR spectrum of (-)-schisantherin E in DMSO-*d*₆

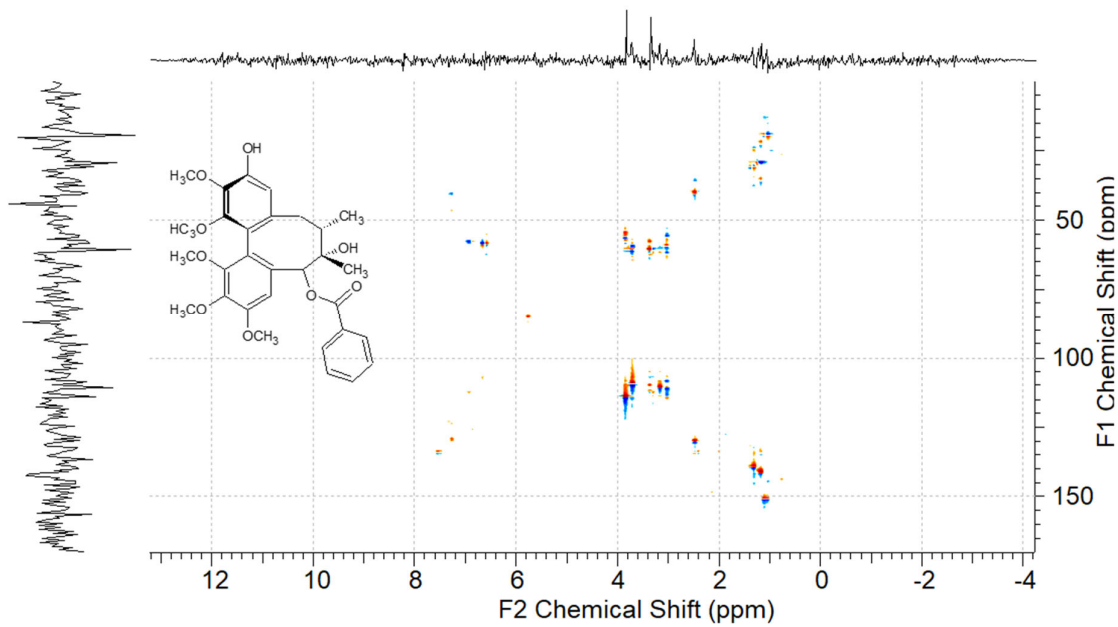


Figure S77. HSQC NMR spectrum of (-)-schisantherin E in $\text{DMSO}-d_6$

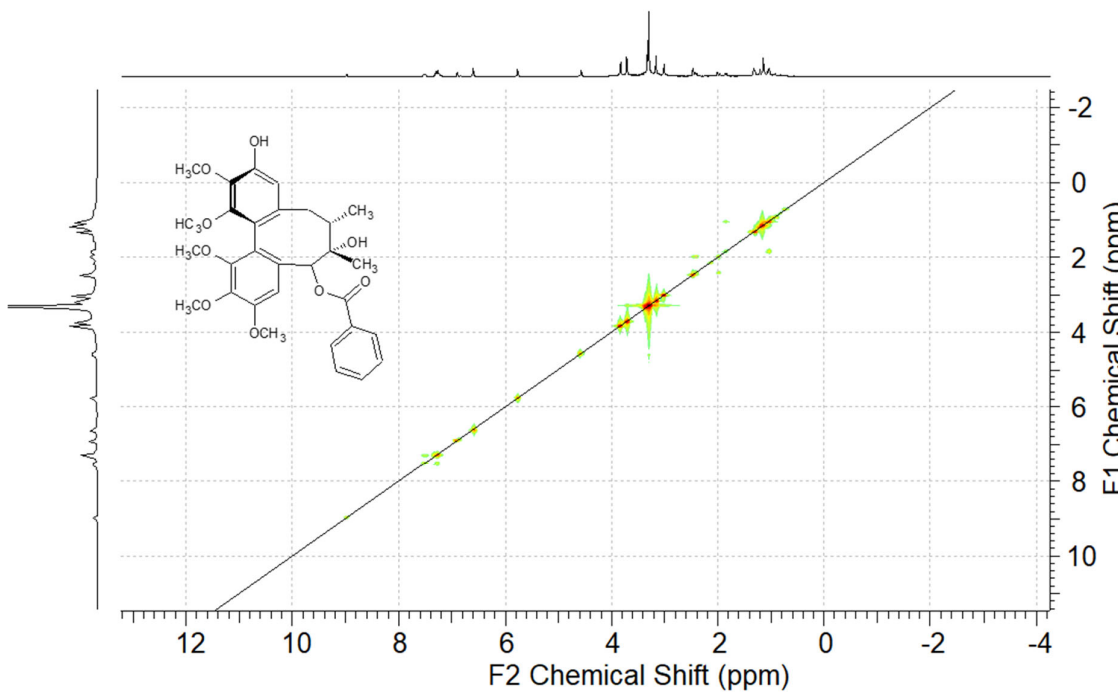


Figure S78. COSY NMR spectrum of (-)-schisantherin E in $\text{DMSO}-d_6$

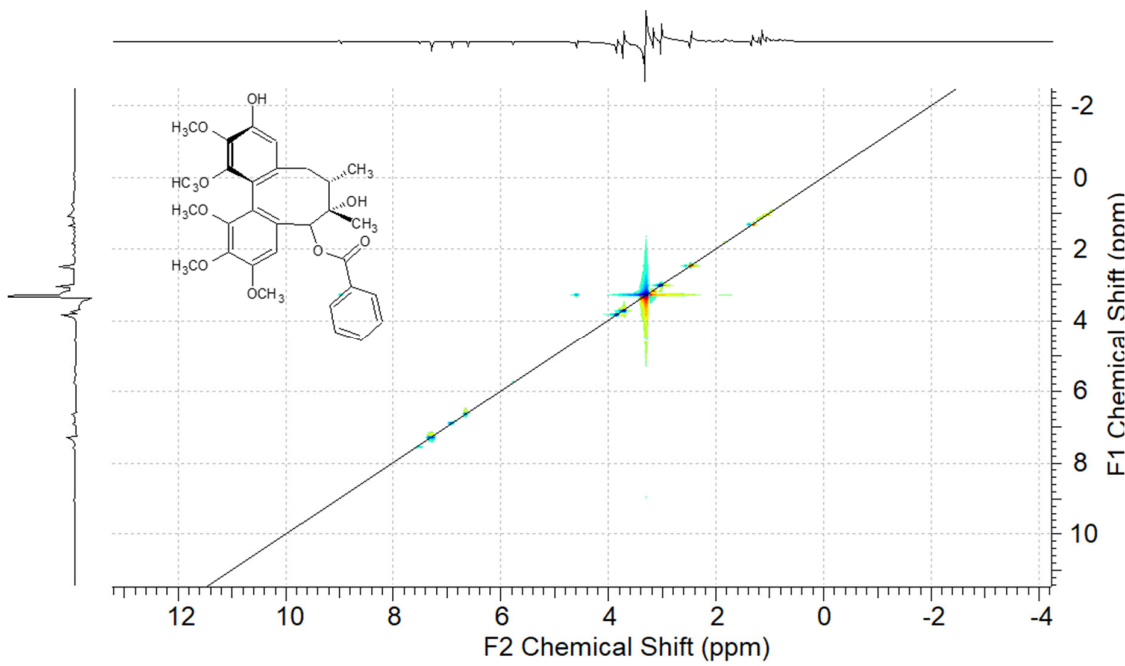


Figure S79. NOESY NMR spectrum of (-)-schisantherin E in $\text{DMSO}-d_6$

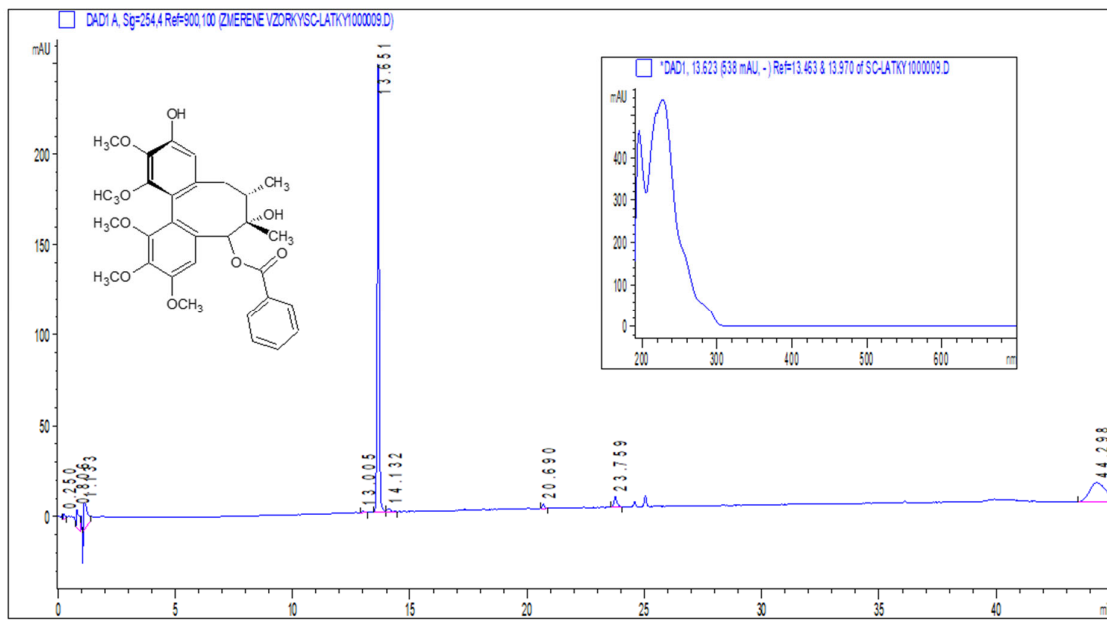


Figure S80. HPLC-DAD chromatogram of (-)-schisantherin E

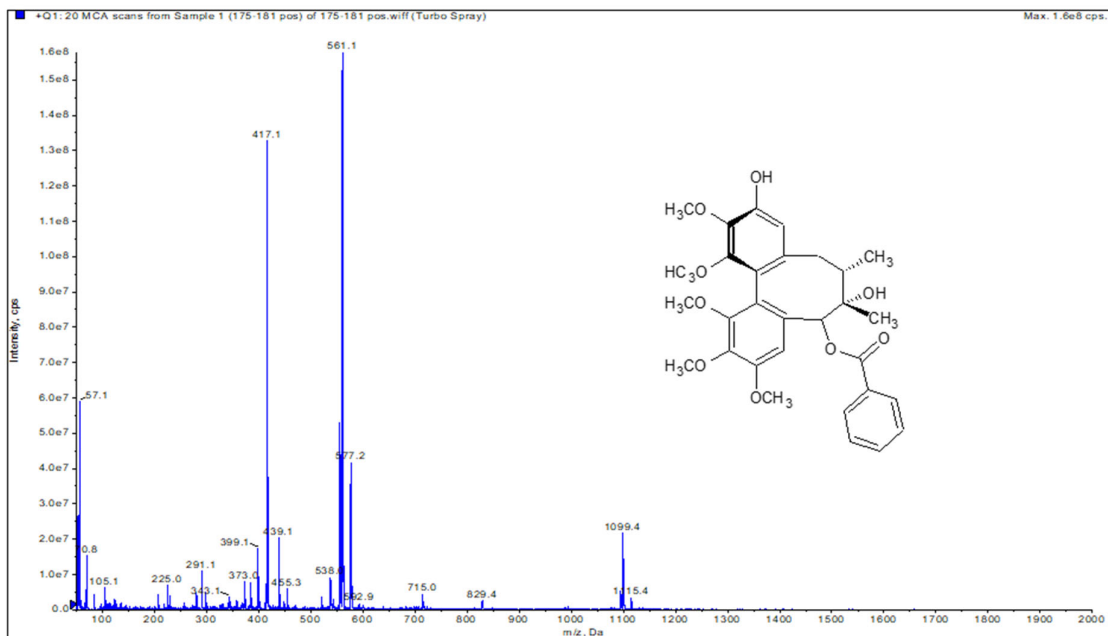


Figure S81. LR-MS spectrum of (-)-schisantherin E

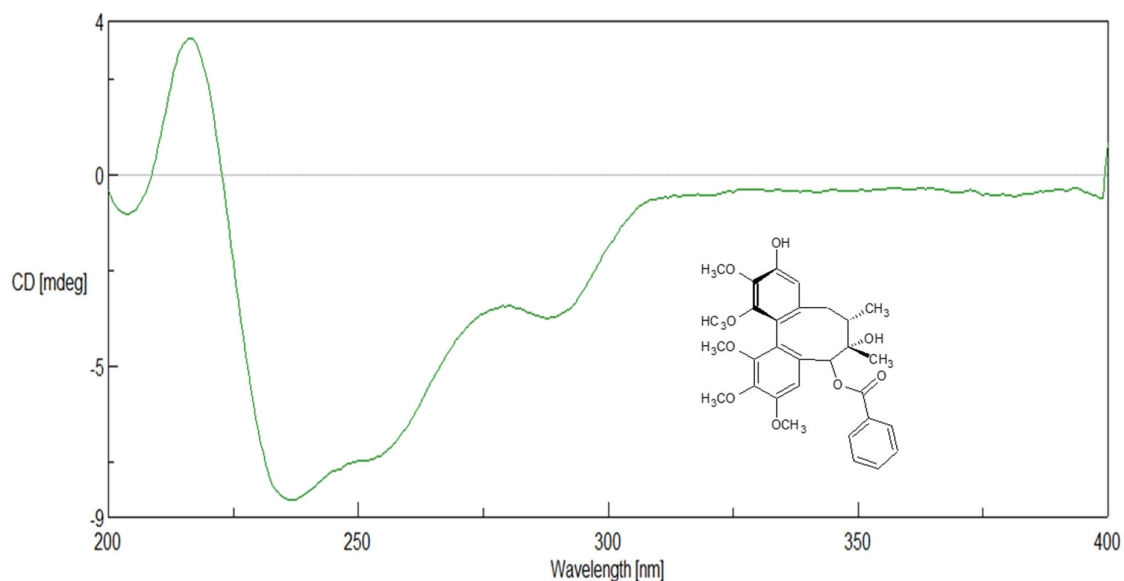


Figure S82. CD spectrum of (-)-schisantherin E in methanol ($c=1 \text{ mg/mL}$)

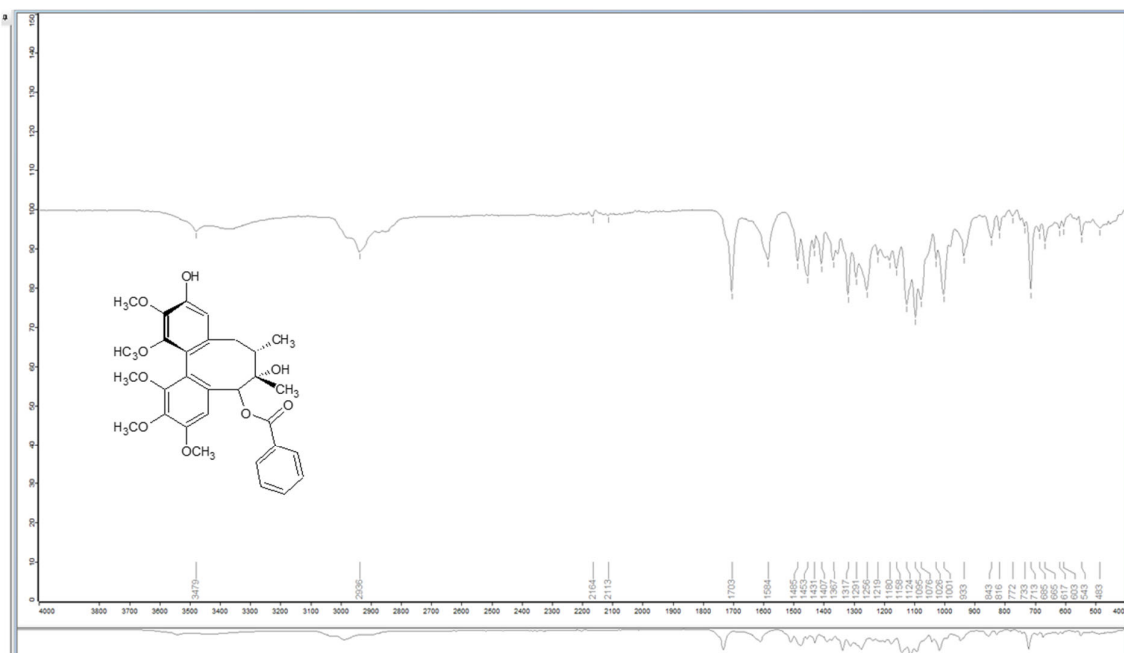


Figure S83. IR spectrum of (-)-schisantherin E

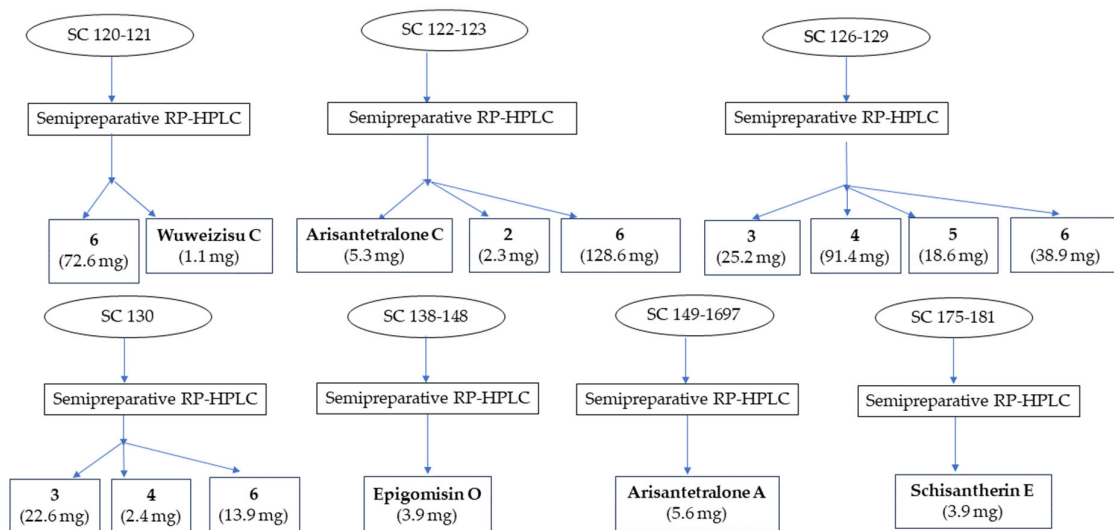


Figure S84. Schema of isolation and total yields of compounds 2–6, (-)-wuweizisu C, arisantetralone A, arisantetralone C, epigomisin O, and (-)-schisantherin E

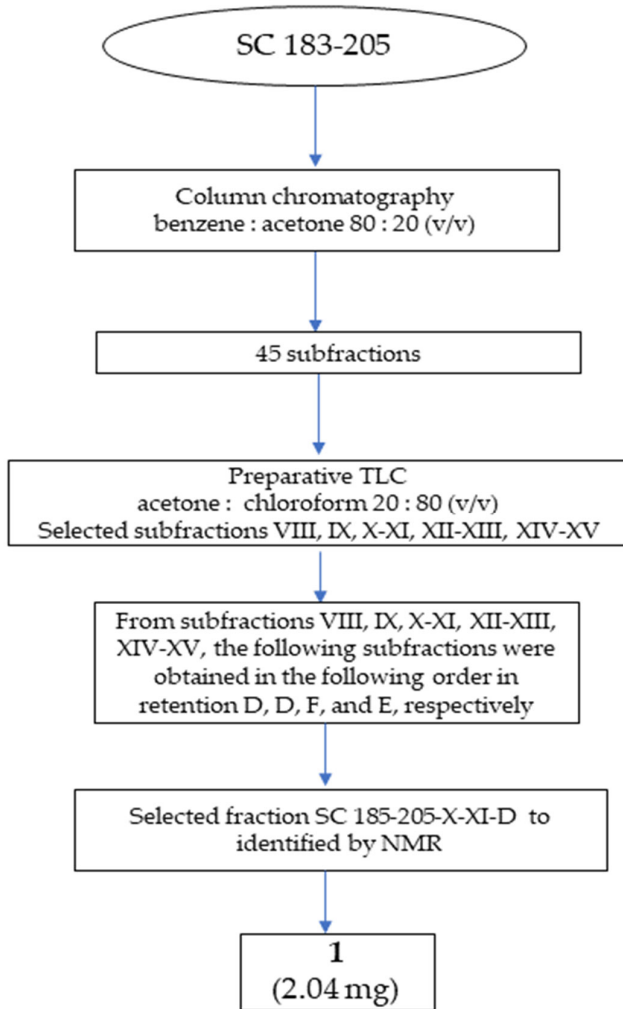


Figure S85. Schema of isolation and yield of compound 1

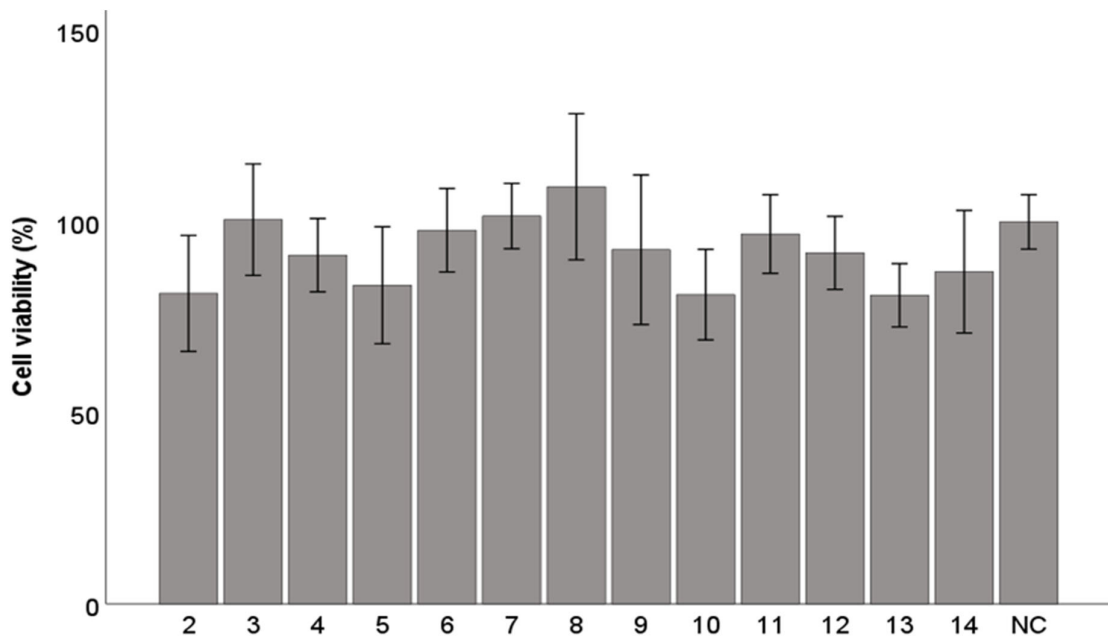


Figure S86. Antiproliferative activity of lignans **2–14**, expressed as % of cell viability. The concentration of tested lignans **2–14** was 10 μ M. DMSO was used as the solvent and was added as the negative control (NC). The results are expressed as the mean \pm SEM for three independent experiments measured in triplicate and are statistically compared to NC using Kruskal-Wallis test.

Table S1. Chromatographic conditions of separation of compounds **2**, **6**, and arisantetralone C from fraction SC 122-123

Stationary phase: Ascentis RP-Amide 25 cm \times 10 mm; 5 μ m (Supelco, USA)

Detection: DAD detector λ = 220; 240; 260; 280 nm

Flow: 5 mL/min

Injection: 40 μ l

Temperature: 40 °C

HPLC Dionex Ultimate 3000 (Thermo Fischer Scientific, USA)

Time (min)	MeOH (%)	ACN (%)	0.2 % HCOOH (%)
0	0	47	53
29.00	0	85	15
29.10	100	0	0
35.00	100	0	0
35.10	0	100	0
40.00	0	100	0
40.10	0	47	53
45.00	0	47	53

Table S2. Chromatographic conditions of separation of compounds **3**, **4**, **5** and **6** from fraction SC 130

Stationary phase: Ascentis RP-Amide 25 cm × 10 mm; 5 µm (Supelco, USA)

Detection: DAD detector $\lambda = 240; 260; 280$ nm

Flow: 5 mL/min

Injection: 15 µL

Temperature: 40 °C

YL9100 (Young-Lin Instruments, South Korea)

Time (min)	MeOH (%)	ACN (%)	0.2 % HCOOH (%)
0	0	50	50
30.00	0	80	20
30.01	0	100	0
35.00	0	100	0
35.01	100	0	0
40.00	100	0	0
40.01	0	50	50
45.00	0	50	50

Table S3. Chromatographic conditions of purification of compound **3** from fraction SC 130

Stationary phase: Ascentis RP-Amide 25 cm × 10 mm; 5 µm (Supelco, USA)

Detection: DAD detector $\lambda = 240; 260; 280$ nm

Flow: 5 mL/min

Injection: 30 µL

Temperature: 40 °C

HPLC Dionex Ultimate 3000 (Thermo Fischer Scientific, USA)

Time (min)	MeOH (%)	ACN (%)	0.2 % HCOOH (%)
0	0	55	45
18.00	0	64	36
18.10	100	0	0
23.00	100	0	0
23.10	0	55	45
28.00	0	55	45

Table S4. Chromatographic conditions of the first purification of compounds **4** and **5** from fraction SC 130

Stationary phase: Ascentis RP-Amide 25 cm × 10 mm; 5 µm (Supelco, USA)

Detection: DAD detector $\lambda = 240; 260; 280$ nm

Flow: 5 mL/min

Injection: 25 µL

Temperature: 40 °C

HPLC Dionex Ultimate 3000 (Thermo Fischer Scientific, USA)

Time (min)	MeOH (%)	ACN (%)	0.2 % HCOOH (%)
0	0	55	45
18.00	0	64	36
18.10	100	0	0
23.00	100	0	0
23.10	0	55	45
28.00	0	55	45

Table S5. Chromatographic conditions of the second purification of compounds **4** and **5** from fraction SC 130

Stationary phase: Ascentis C18 25 cm × 10 mm, 5 µm (Supelco, USA)

Detection: DAD detector $\lambda = 220, 240; 260; 280$ nm

Flow: 5 mL/min

Injection: 10 µL

Temperature: 40 °C

HPLC Dionex Ultimate 3000 (Thermo Fischer Scientific, USA)

Time (min)	MeOH (%)	ACN (%)	0.2 % HCOOH (%)
0	60	0	40
18.00	73	0	27
18.10	0	100	0
23.00	0	100	0
23.10	60	0	40
28.00	60	0	40

Table S6. Chromatographic conditions of separation of compound **6** and (-)-wuweizisu C from fraction SC 120-121

Stationary phase: Ascentis RP-Amide 25 cm × 10 mm; 5 µm (Supelco, USA)

Detection: DAD detector $\lambda = 220; 240; 260; 280$ nm

Flow: 5 mL/min

Injection: 10 µL

Temperature: 40 °C

System YL9100 (Young-Lin Instruments, South Korea)

Time (min)	MeOH (%)	ACN (%)	0.2 % HCOOH (%)
0	0	30	70
30.00	0	80	20
30.01	0	100	0
35.00	0	100	0
35.01	100	0	0
40.00	100	0	0
40.01	0	30	70
45.00	0	30	70

Table S7. Chromatographic conditions of separation of epigomisin O from fraction SC 138-148

Stationary phase: Ascentis RP-Amide 25 cm × 10 mm; 5 µm (Supelco, USA)

Detection: DAD detector $\lambda = 220, 240, 260, 280$ nm

Flow: 5 mL/min

Injection: 25 µL

Temperature: 40 °C

HPLC Dionex Ultimate 3000 (Thermo Fischer Scientific, USA)

Time (min)	MeOH (%)	ACN (%)	0.2 % HCOOH (%)
0	60	0	40
20.00	79	0	21
20.10	0	100	0
28.00	0	100	0
28.10	100	0	0
36.00	100	0	0
36.10	60	0	40
45.00	60	0	40

Table S8. Chromatographic conditions of separation of arisantetralone A from fraction SC 149-167

Stationary phase: Ascentis RP-Amide 25 cm × 10 mm; 5 µm (Supelco, USA)

Detection: DAD detector $\lambda = 240, 260, 280$ nm

Flow: 5 mL/min

Injection: 10 µL

Temperature: 40 °C

System YL9100 (Young-Lin Instruments, South Korea)

Time (min)	MeOH (%)	ACN (%)	0.2 % HCOOH (%)
0	0	40	60
20.00	0	60	40
20.01	0	100	0
25.00	0	100	0

25.01	100	0	0
30.00	100	0	0
30.01	0	40	60
45.00	0	40	60

Table S9. Chromatographic conditions of separation of (-)-schisantherin E from fraction SC 175-181

Stationary phase: Ascentis RP-Amide 25 cm × 10 mm; 5 µm (Supelco, USA)

Detection: DAD detector $\lambda = 240, 260, 280$ nm

Flow: 5 mL/min

Injection: 20 µL

Temperature: 40 °C

system YL9100 (Young-Lin Instruments, South Korea)

Time (min)	MeOH (%)	ACN (%)	0.2 % HCOOH (%)
0	0	30	70
30.00	0	90	10
30.01	0	100	0
35.00	0	100	0
35.01	100	0	0
40.00	100	0	0
40.01	0	30	70
45.00	0	30	70

Table S10. Chromatographic conditions of separation of compounds **3**, **4**, **5**, and **6** from fraction SC 126-129

Stationary phase: Ascentis RP-Amide 25 cm × 10 mm; 5 µm (Supelco, USA)

Detection: DAD detector $\lambda = 220, 240, 260, 280$ nm

Flow: 5 mL/min

Injection: 15 µL

Temperature: 40 °C

HPLC Dionex Ultimate 3000 (Thermo Fischer Scientific, USA)

Time (min)	MeOH (%)	ACN (%)	0.2 % HCOOH (%)
0	0	40	60
29.00	0	81	19
29.10	100	0	0
35.00	100	0	0
35.10	0	100	0
40.00	0	100	0
40.10	0	40	60
45.00	0	40	60

Table S11. Chromatographic conditions of purification of compounds **4** and **5** from fraction SC 126-129

Stationary phase: Ascentis C18 25 cm × 10 mm, 5 µm (Supelco, USA)

Detection: DAD detector $\lambda = 220, 240; 260; 280$ nm

Flow: 5 mL/min

Injection: 15 µL

Temperature: 40 °C

HPLC Dionex Ultimate 3000 (Thermo Fischer Scientific, USA)

Time (min)	MeOH (%)	ACN (%)	0.2 % HCOOH (%)
0	70	0	30
19.00	82.9	0	17.1
19.10	0	100	0
24.00	0	100	0
24.10	70	0	30
29.00	70	0	30